AEDC-TR-68-46

cy 1

ANGULAR DISTRIBUTION OF RADIATION REFLECTED FROM CARBON DIOXIDE CRYODEPOSITS FORMED ON 77°K SURFACES

Thermal Radiation Section

ARO, Inc.

April 1968

AEROSPACE ENVIRONMENTAL FACILITY
ARNOLD ENGINEERING DEVELOPMENT CENTER
AIR FORCE SYSTEMS COMMAND
ARNOLD AIR FORCE STATION, TENNESSEE

NOTICES

When U. S. Government drawings specifications, or other data are used for any purpose other than a definitely related Government procurement operation, the Government thereby incurs no responsibility nor any obligation whatsoever, and the fact that the Government may have formulated, furnished, or in any way supplied the said drawings, specifications, or other data, is not to be regarded by implication or otherwise, or in any manner licensing the holder or any other person or corporation, or conveying any rights or permission to manufacture, use, or sell any patented invention that may in any way be related thereto.

Qualified users may obtain copies of this report from the Defense Documentation Center.

References to named commercial products in this report are not to be considered in any sense as an endorsement of the product by the United States Air Force or the Government.

ANGULAR DISTRIBUTION OF RADIATION REFLECTED FROM CARBON DIOXIDE CRYODEPOSITS FORMED ON 77°K SURFACES

Thermal Radiation Section

ARO, Inc.

AF - AEDC
Arnold AFS Tenn

FOREWORD

The research reported herein was sponsored by Headquarters, Arnold Engineering Development Center (AEDC), Air Force Systems Command (AFSC), Arnold Air Force Station, Tennessee, under Program Element 6240533F, Project 8951, Task 895104.

The results of the research were obtained by ARO, Inc. (a subsidiary of Sverdrup & Parcel and Associates, Inc.), contract operator of AEDC, AFSC, under Contract AF40(600)-1200. The work was performed under ARO Project No. SW5703 and SW5803, and the manuscript was submitted for publication on January 31, 1968.

The experimental apparatus employed in this investigation was set up by B. A. McCullough, and the experimental data reported herein were obtained by Peter Mueller. The report was prepared by K. E. Tempelmeyer, Peter Mueller, and A. M. Smith, with the assistance of several people at the Aerospace Environmental Facility.

This technical report has been reviewed and is approved.

Terry L. Hershey
Captain, USAF
Research Division
Directorate of Plans
and Technology

Edward R. Feicht
Colonel, USAF
Director of Plans
and Technology

ABSTRACT

The angular distribution of light reflected from carbon dioxide cryodeposits formed at various rates on polished copper and black substrates has been measured for various cryodeposit thicknesses and angles of incidence. Cryodeposits were found to reflect light essentially diffusely at thicknesses greater than about 100 microns (μ). The specular reflection from both polished copper and black substrates could be reduced by as much as two orders of magnitude by a 100-μ-thick cryodeposit. Bragg interference, backscattering, scattering interference, and shifts of the angular location of the specular component were all observed and illustrated that light reflection from cryodeposits is a very complex phenomenon.

CONTENTS

TABLES

APPENDIX

Illustrations

NOMENCLATURE

$E(\psi, \theta, \tau)$	Reflected energy at angle θ for an arbitrary incidence angle, cryodeposit thickness, and ϕ = 0 deg
$E(\psi, \psi, 0)$	Energy at specular angle of reflection from the substrate without a cryodeposit and ϕ = 0 deg
E_i	Energy of incident light
E_r	Energy of reflected light
t	Time
Δt	Time between adjacent peaks in Bragg interference pattern
$\Delta\theta$	Angular shift of specular peak
$\Delta\tau$	Change in cryodeposit thickness between adjacent peaks in Bragg interference patterns
$\Delta\omega_i$	Solid angle of incident radiation
$\Delta\omega_r$	Solid angle of reflected radiation
θ	Angle of reflected light from the substrate normal
θ_{peak}	Angle of shifted reflected specular peak
λ	Wavelength

μ	Refractive index
τ	Cryodeposit thickness
ϕ	Azimuthal angle of reflected light
ψ	Angle of incident light from the substrate normal

SECTION I
INTRODUCTION

Most large thermal-vacuum space simulation chambers employ cryogenic pumping, and consequently, the test vehicle is surrounded by panels cooled to near 77°K by liquid nitrogen (LN_2). These panels are normally painted black to minimize the reflection of radiation from the solar simulator. However, as carbon dioxide (CO_2) and water (H_2O) vapor frost films form on the panel, caused by cryopumping, the reflective characteristics of the panels change, and the test vehicle thermal balance would be altered. For these reasons the reflective characteristics of cryodeposits are being systematically investigated at the Aerospace Environmental Facility (AEF). References 1 through 7 report some of the reflectance properties of CO_2 and H_2O cryodeposits which have been obtained to date. The wavelength range covered in these studies is that of most interest in simulating the solar spectrum.

One phase of this program is the measurement of the angular distribution of light reflected from cryodeposits. This report presents data showing the distribution of reflected radiation from thin CO_2 cryodeposits formed on polished copper and black substrates. Cryodeposit thicknesses vary from approximately 1 to approximately 270 microns (μ). For all tests the incident light beam was provided by a xenon arc lamp, oriented at angles from 0 to 70 deg from the normal to the substrate. Test results presented herein are useful in determining the effect of wall reflections on the thermal balance of test vehicles in space chambers and also contribute to the knowledge of the structure of cryodeposits.

SECTION II
EXPERIMENTAL APPARATUS

2.1 VACUUM CHAMBER

All tests were conducted in a 30-in.-diam spherical vacuum chamber, schematically shown in Fig. 1 (Appendix). It was assembled from two flanged 30-in. stainless steel hemispheres joined with an O-ring seal. The pumping system consisted of a 400-liter/min mechanical pump and a 6-in. oil diffusion pump which was equipped with a water-cooled baffle and an LN_2-cooled cold cap. A vacuum-rated valve was used to isolate the chamber from the pumping system. The system could be pumped to 1×10^{-6} torr. The interior of the chamber

was painted with flat black paint to minimize the reflection of radiation from the chamber walls.

2.2 TEST SURFACE

Test cryodeposits were formed on a 7.6- by 10.2-cm copper cryosurface which was located near the center of the chamber (Fig. 1). It could be cooled to 77°K by the use of LN_2. A rotary vacuum seal was used to allow rotation of the surface to any desired polar angle with respect to the incident light beam. The position of the surface was set to ±0.5 deg by means of a protractor indexing device. Cryodeposits were formed on a polished copper surface with an rms surface roughness of 0.01 μ or on a black epoxy-coated surface (Cat-A-Lac Black®). The surface roughness of the black painted surface was not determined.

2.3 OPTICAL SYSTEM AND DETECTOR

The optical system consisted of a 1600-watt xenon lamp, a condensing lens system, and a collimating tube which was built into the chamber port. A schematic of the optical system is given in Fig. 2. The chamber was also equipped with a detector arm having a 25-cm radius on which silicon solar cells were mounted at 10-deg intervals. The arm could be remotely rotated at constant angular velocity about the test surface, thereby mapping the distribution of the reflected radiation. A composite normalized spectral distribution of the xenon lamp, beam collimating system, and detector is presented in Fig. 3. Data in Fig. 3 were obtained by removing the cryosurface from the chamber, aligning the detector to intercept the light beam, and measuring the maximum detector output as different interference-type filters were inserted.

2.4 GAS ADDITION SYSTEM

Carbon dioxide with a purity level of 99.8 percent was introduced into the vacuum sphere by means of a calibrated leak system. The gas was supplied by a reservoir which was maintained at an essentially constant forepressure of 760 torr and flowed into the chamber through a needle valve and through one of three leaks. The three available leaks were calibrated at the operating forepressure and at backpressures spanning the range covered in the experiment.

Cryodeposits of various thicknesses were formed on the LN_2-cooled test surface by allowing CO_2 to flow into the chamber for various time

intervals from 1 min to several hours (depending on the flow rate of the leak). The thickness of the cryodeposit was determined by the method outlined in Section III.

2.5 INSTRUMENTATION

The chamber pressure was measured with a conventional ionization gage or an Alphatron®, depending on the test pressure level, and the forepressure on the leak was read on a Wallace-Tiernan gage. For most tests the cryosurface temperature was monitored by means of a conventional thermocouple.

As the cryodeposit formed, the detector output was recorded continuously on a conventional time-history plotter. Distributions of reflected light from a given deposit were recorded on an X-Y plotter.

SECTION III
PROCEDURE

The angular distribution of light reflected from the surfaces was determined by the biangular technique, illustrated in Fig. 4. Incident energy, E_i, contained in the solid angle, $\Delta\omega_i$, was directed onto the test surface at the angle, ψ, from the normal. Reflected energy, E_r, in a particular solid angle, $\Delta\omega_r$, would lie at an angle, θ, from the normal and the angle, ϕ, from the plane of incidence. The detector arm was arranged so that its rotation mapped the reflected energy over all angles of θ for ϕ = 0, 10, 20 deg, etc.* However, only those distributions obtained for ϕ = 0 deg will be presented inasmuch as the distributions for $\phi > 0$ deg demonstrated nothing unusual.

3.1 DISTRIBUTION MEASUREMENTS

After the chamber had been pumped to about 1 x 10^{-6} torr and valved off from the pumping system, the xenon lamp was turned on and the test surface rotated to the desired angle with respect to the incident light beam. For tests where the incident light was normal to the test surface, alignment was achieved by rotating the surface until

*Detectors mounted at 10-deg intervals on the rotating arm provided the various angles of ϕ.

the reflection patterns were symmetrical. For nonnormal incident radiation, the incidence angle was approximately set with a protractor indexing device.

With the test surface still at room temperature, the detector arm was rotated through an arc of about 90 to -60 deg with respect to the surface normal and a reference trace of angular distribution of reflected light made for the surface without a cryodeposit ($\tau = 0$). The test surface was rotated to different values of ψ and the mapping procedure repeated. Next, the cryosurface was cooled to 77°K. Before CO_2 was admitted into the chamber, another reference trace of reflected light was usually made again for various values of ψ. If the chamber had been pumped to at least 1×10^{-6} torr, these two reference traces were essentially identical. At higher background pressures, slight differences occurred because the residual CO_2 and H_2O in the chamber formed a thin film on the test surface.

Cryodeposit films were then formed by flowing CO_2 into the chamber, through the desired leak, for a specified time. Usually, the detector was set at the specular angle ($\psi = \theta$), and the specular component of the reflected radiation was monitored continuously as the cryodeposit grew. After the flow was stopped and CO_2 was cryopumped on the test surface, producing a layer of a given thickness, the angular distribution of reflected light was again recorded for various values of ψ. Carbon dioxide was again added to the chamber forming another layer on top of the first, and the above radiation measurements were repeated. This procedure was continually repeated and measurements made for each resulting cryodeposit thickness. Previous tests reported in Ref. 7 have demonstrated that the angular distributions of light reflected from multilayered cryodeposits like those formed in these tests are the same as those from cryodeposits which are formed in a continuous manner.

3.2 CRYODEPOSIT THICKNESS MEASUREMENTS

The cryodeposit thickness was determined by measuring the thickness growth rate by means of Bragg Refraction-Reflection interference phenomena; the technique is discussed in some detail in Ref. 7. These measurements were made separately for each flow leak used in the study by setting the angle of incidence of the light beam, ψ, to some desired value. The detector arm was then rotated to the angle of specular reflection ($\psi = \theta$) and left in that position. An interference-type filter (usually $\lambda \simeq 0.9\,\mu$) was inserted into the light beam. Then the cryosurface was cooled with LN_2, and with the chamber valved off from the

pumping system, CO_2 was bled in at a constant rate through the desired leak. The variation of the intensity of the reflected light was monitored continuously at the specular angle of reflection. As the cryodeposit thickness increases, Bragg interference occurs. Rays which are (1) reflected from the CO_2 cryodeposit surface and (2) reflected from the substrate* are alternately in and out of phase with each other. Thus, a detector set at the specular angle of reflection then experiences a varying signal such as shown in Fig. 5. From the Bragg equation it is apparent that the change in cryodeposit thickness between two adjacent peaks is given by:

$$\Delta r = \frac{\Delta q \lambda}{2\mu \sqrt{1 - \frac{\sin^2 \theta}{\mu^2}}} \tag{1}$$

where $\Delta q \equiv 1$. Values of the refractive index, μ, for CO_2 cryodeposits are given in Ref. 7. Because the gas addition rate to the chamber is essentially constant, the cryodeposit grows at a constant rate:

$$\frac{dr}{dt} = \text{constant} \tag{2}$$

This is demonstrated by an essentially constant spacing between adjacent peaks or valleys in the test results shown in Fig. 5.

The change in thickness per period (i.e., between adjacent peaks) is given by Eq. (1), and the period Δt can be obtained from the test data (Fig. 5, for example). Since the growth rate is constant, the overall cryodeposit thickness may be determined by measuring the flow time from:

$$r = \frac{\Delta r}{\Delta t} t = \frac{t}{\Delta t} \frac{\lambda}{2 \mu \sqrt{1 - \frac{\sin^2 \theta}{\mu^2}}} \tag{3}$$

This procedure was repeated for each leak. The growth rate, $\Delta r / \Delta t$, for each leak employed is given below:

Leak	Cryodeposit Growth Rate, μ/min
1	2.25
2	0.423
3	0.0385

*Data shown in Fig. 5 were obtained with a Cat-A-Lac Black substrate, but the same type of patterns also occurs for the polished copper substrate.

The spectrum of the xenon lamp exhibits a rather strong peak at wavelengths near 0.9 μ (see Fig. 3). As a result, weaker Bragg interference also occurred even without the use of filters for thin layers. Usually, these patterns were recorded as the test cryodeposits were being formed to provide a check on the thickness determined from Eq. (3). In all cases the agreement was good.

SECTION IV
RESULTS

The distribution of light reflected from CO_2 cryodeposits of various thicknesses on a polished copper substrate is presented in Figs. 6, 7, and 8. Table I summarizes the test conditions for which these distribution measurements were made.

TABLE I
TEST RESULTS FOR A POLISHED COPPER SUBSTRATE

Figure Number	Substrate	ψ, deg	Range of θ, deg	Cryodeposit Formation Rate, μ/min	Cryodeposit Thickness, μ
6	Polished Copper	10, 20, 30, 40, 50, 60, 70	-30 to +90	2.25	0, 2.25, 6.75, 15.75, 20.25, 27.0, 33.75, 50.63, 67.5, 122.5, 157.5, and 270.0
7	Polished Copper	10, 20, 30, 40, 50, 60, 70	0 to +90	0.423	0, 12.7, 25.4, and 50.8
8	Polished Copper	10, 20, 30, 40, 50, 60, 70	-90 to +75	0.0385	0, 1.5, 3.5, and 7.5

The distribution of light reflected from CO_2 cryodeposits formed on a black epoxy substrate* is given in Figs. 9, 10, and 11. Test

*Cat-A-Lac Black

conditions at which these distributions were measured are summarized in Table II.

TABLE II
TEST RESULTS FOR A BLACK EPOXY PAINT

Figure Number	Substrate	ψ, deg	Range of θ, deg	Cryodeposit Formation Rate, μ/min	Cryodeposit Thickness, μ
9	Black* Epoxy Paint No. 1	0, 10, 20, 30, 40, 50, 60, 70	-50 to +90	2.25	0, 2.25, 6.75, 15.75, 33.75, 67.50, 157.50, and 270.0
10	Black* Epoxy Paint No. 1	0, 10, 20, 30, 40, 50, 60, 70	-45 to +90	0.423	0, 2.25, 4.50, 15.67, 38.20, and 76.20
11	Black* Epoxy Paint No. 2	0, 10, 20, 30, 40, 50, 60, 70	-50 to +90	0.0385	0, 1.46, 2.25, 6.75, 15.75, and 24.75

Except for data given by Fig. 8, the distributions of reflected light are presented in normalized form, and all data presented are for $\phi = 0$ deg. The normalization was achieved by dividing the detector output, which is a function of ψ, θ, and τ, or $E(\psi, \theta, \tau)$, by the specular reflectance of the substrate without a cryodeposit (i.e., $\tau = 0$ and $\theta = \psi$) or:

$$\text{Normalized Value} = \frac{E(\psi, \theta, \tau)}{E(\psi, \psi, 0)}$$

The normalizing factors, $E(\psi, \psi, 0)$, are given in Fig. 12 for each incidence angle for the polished copper and the two different paint coatings.* If desired, the measured distributions of reflected light may be reproduced by multiplying the normalized distributions by the appropriate normalizing factor from Fig. 12. Several methods of data presentation are employed in Figs. 7 through 11.

As the detector arm passed the angle $-\theta \cong \psi$, it blocked off the incident light beam, and the signal fell to zero (see Fig. 6, for example). For distributions measured with the black substrate, it was possible to interpolate across these blockage-induced "valleys" with confidence. When interpolation was employed, the range of interpolation is identified in the figure.

*Data were obtained with two different black painted surfaces. Since the reflection properties of the paint were found to vary from batch to batch, the two layers are identified as coatings 1 and 2.

SECTION V
DISCUSSION

5.1 REFLECTION FROM THIN CRYODEPOSITS

If the light source has a strong energy peak in some wavelength range (i. e., if it is quasi-monochromatic), the overall level of the reflected distribution is significantly influenced by Bragg interference when the cryodeposits are relatively thin. Figure 13 gives the signal variation (proportional to the cryodeposit reflectance) as a function of cryodeposit thickness for "white" light from the xenon lamp having an incidence angle of 30 deg. Large variations of the amount of reflected energy are observed until the cryodeposit is about 2 μ thick. The overall level of the reflected distributions follows the same variation shown here. If the effect of this interference phenomenon is not considered, the distributions would give the appearance of being inconsistent when the cryodeposits are quite thin. A good example of this may be observed by comparing the distributions obtained for τ = 1.465 and 2.25 μ in Fig. 11. The overall energy level for these two distributions, however, is quite understandable, at least at ψ = 30 deg, with the aid of Fig. 13.

The effect of Bragg interference phenomena on the level of the reflected distributions may produce an important effect in thermal-vacuum tests. Any solar simulator which reasonably well approximates the solar spectrum would be sufficiently monochromatic to produce Bragg interference. Thus, the wall reflectance could be expected to vary by a factor of four or five until the cryodeposit achieved a thickness of about 2 μ. Moreover, since the wall reflectance is quite sensitive to small changes in cryodeposit thickness in this range, the introduction of relatively small amounts of CO_2 into the chamber by the test vehicle or by other means could significantly change the wall reflectance. It should be noted that these changes could be beneficial in that the wall reflectance may be reduced.

The extent of this effect depends on how monochromatic the light source is. This effect also exists for a polished copper substrate but to a much lesser degree (see Ref. 7).

5.2 ANGULAR DISTRIBUTION OF REFLECTED LIGHT

Measurements made in an integrating sphere, which have been reported previously (Ref. 5), have shown that the hemispherical reflectance of the substrate (without a cryodeposit) is initially decreased

as a CO_2 cryodeposit begins to form. When the cryodeposit reaches a thickness from about 100 to 400 μ, the hemispherical reflectance then begins to increase with further increases of the cryodeposit thickness. In the case of a black substrate, the amount of light reflected from a cryodeposit can be several times that reflected from the substrate alone. The same trends are evident in the angular distribution of reflected light data presented in Figs. 6 through 11. The amount of light reflected at the specular angle is significantly decreased with increasing cryodeposit thickness for all angles of incidence. For example, a 100-μ-thick CO_2 cryodeposit on a polished copper substrate reflects about 1/100 as much light at the specular angle than does the substrate without a cryodeposit. Inspection of the angular distributions shows, however, the amount of light reflected at most other angles is significantly increased. Thus, in general, the cryodeposit has a diffusing effect, at least over the wavelength range covered in this investigation. The specular component of the reflected light decreases with increasing cryodeposit thickness and eventually disappears completely, whereas the diffuse components, in general, steadily increase. The details of these changes, however, vary somewhat between the two substrates investigated.

5.2.1 Polished Copper Substrate

Figure 6 contains the most complete set of angular distributions of light reflected from cryodeposits formed on a copper substrate. The polished copper substrate itself was a highly specular reflector at all incident angles. Nearly all of the reflected energy was within ±5 deg of the specular angle. Also, the copper surface reflected about the same amount of light at all incident angles (Fig. 12).

As the cryodeposit thickness increased, the specular component of the reflected light decreased rapidly. At a thickness of 67.5 μ and greater, the specular component disappeared completely for all incident angles except ψ = 70 deg. This was initially accompanied by an increased amount of reflected radiant energy at nonspecular angles. For thicker deposits the amount of light reflected at all angles appeared to decrease steadily.* The thicker layers (122 and 270 μ) appeared to be quasi-diffuse and reflected a small amount of light in all directions in the plane of incidence and specular reflection (ϕ = 0 deg). Other

*Previous test results obtained in an integrating sphere (Ref. 5) demonstrated that the reflectance of CO_2 cryodeposits on a polished stainless steel substrate begins to increase at thicknesses between about 300 and 400 μ. Layers this thick were not studied in the present investigation.

detectors located at 10-deg intervals on the rotating arm (i.e., ϕ = 10, 20 deg, etc.) indicated that nothing unexpected occurred outside of the primary ϕ = 0 deg measuring plane.

The effect of the cryodeposit formation rate on the angular distribution of reflected light with copper substrates may be observed by comparing the distributions given in Figs. 6 and 7. At formation rates of 2.25 and 0.423 μ/min, respectively, the general trends in the distributions are seen to be similar; that is, there was a rapid decrease and eventual disappearance of the specular peak resulting in a quasi-diffuse distribution of reflected light. The general level of the quasi-diffuse reflected energy from about a 50-μ-thick layer was about the same for both formation rates at all angles of incidence. On the copper substrate there appeared to be little effect of these two formation rates on the reflection properties of the cryodeposits.

5.2.2 Black Substrate

The black substrate had an overall reflectivity of about 5 to 8 percent. With no cryodeposit, it exhibited a quite broad specular peak at all angles of the incident light (see Fig. 9). The black epoxy-coated surface reflected considerably more light at large incident angles from the normal. For example, coating 1 reflected almost 10 times as much light at ψ = 70 deg as it did at ψ = 10 deg (see Fig. 12).

It may be observed in Fig. 9 that as the cryodeposit grows on the black surface, the specular component of the reflected light decreases rapidly and finally disappears at thicknesses of about 67.5 μ and above for the lower incident angles. At an incident angle of 70 deg a weak specular component is estimated to exist at thicknesses up to 100 μ. The thicker layers examined, τ = 157.5 and 270 μ, appeared to reflect light quite diffusely at all angles of incidence (Fig. 9). However, except for ψ = 0 deg, the amount of light reflected in the vicinity of θ = 0 deg was somewhat lower than would be expected from a diffuse distribution. This gives the impression that a significant amount of backscattering occurs along the incident beam. This is also suggested by several of the logarithmic plotted distributions for thin deposits on a copper surface given in Fig. 8.

Figure 9 also illustrates the minimum reflectance at the specular angle is reached, in this case at a thickness of about 67.5 to 100 μ, further increase of the cryodeposit thickness greatly increases the amount of light reflected at all angles. For example, at the lower angles of incidence, increasing the deposit thickness from 67.5 to

270 μ increases the amount of light reflected at all angles by a factor of ten. The change of reflection properties of cryodeposits with thickness is the subject of the next section.

Comparison of Figs. 9, 10, and 11 indicates that the rate of cryodeposit formation has some effect on the distribution of reflected light. This comparison is not too meaningful because the distributions shown were obtained with two different Cat-A-Lac Black coatings. A more direct comparison is made in Fig. 14 where the normalized detector output at the specular angle only is shown as a function of cryodeposit thickness for all three deposit formation rates and for the paint coatings 1 and 2 at the highest formation rate. Different normalizing factors were employed for each coating as shown in Fig. 12. Comparison of the curves in Fig. 14 illustrates that the two paint coatings did reflect light somewhat differently, but if this is taken into account it still appears as if the formation rate does affect the reflection properties of cryodeposits. Only a few cryodeposit thicknesses formed at the slowest rate were investigated because of the long times needed to form the layer. However, these data lead to the conjecture that if the cryodeposit is formed slowly on a black substrate, much thicker layers would be required before the specular component would disappear and before the light would be reflected in a diffuse manner. This suggests then that slowly formed layers may tend to be much smoother. It should be pointed out that the equilibrium chamber pressure was also different for each formation rate (being higher for the larger rates of formation). It is conceivable that this could also have produced the differences shown in Fig. 14. However, measurements of the refractive index of CO_2 cryodeposits made at various pressure levels but at the same formation rate (Ref. 7) indicate that the cryodeposit structure is not drastically different when it is formed at pressures between 10^{-4} to 10 torr. Consequently, it is believed that variation of the background pressure is probably not responsible for the differences shown in Fig. 14.

5.3 EFFECT OF CRYODEPOSIT THICKNESS

The amount of light reflected at the specular angle (i. e., $\theta = \psi$) is shown in Figs. 15 and 16 for cryodeposits of various thicknesses formed on a polished copper and black substrate, respectively. These figures illustrate the decrease of the specular component with increasing cryodeposit thicknesses described previously.

Another comparison of the amount of light reflected at the specular angle ($\psi = \theta = 30$ deg) from deposits on copper and black substrates is given in Fig. 17. It is observed that at the specular angle the amount of light reflected from a polished copper substrate is decreased about

two orders of magnitude, and with a black surface the decrease is about an order of magnitude. One interesting comparison shows that at $\psi = \theta = 30$ deg the amount of light reflected from a 100-μ-thick cryodeposit on a polished copper surface is about the same as would occur if the surface had been painted black.

The present data, together with those given in Ref. 5, indicate that thin CO_2 cryodeposits can be useful in significantly reducing both the specular component and the total amount of light reflected from a cryosurface. In addition, the reflectivity of a black surface can be further decreased by forming a CO_2 cryodeposit about 100 μ thick on it at least for light at wavelengths covered in these tests. In the specular direction this decrease can be as large as an order of magnitude. Figure 17 also illustrates the magnitude of Bragg interference effects with polished copper and black substrates.

5.4 SHIFT OF THE SPECULAR COMPONENT

Another phenomenon which is apparent with a black substrate but not with a copper substrate is that the maximum amount of light reflected from cryodeposits at the higher incidence angles does not occur at the specular angle (see Figs. 9 to 11 for $\psi = 60$ and 70 deg). The amount of this specular shift is illustrated in Fig. 18 where $\Delta\theta$ is defined as

$$\Delta\theta \equiv \theta_{peak} - \psi$$

Without a cryodeposit the specular peak occurred at a little less than 70 deg, which was undoubtedly because of a slight misalignment of the incident beam with respect to the surface. As the cryodeposit thickness was increased from about 2 to 75 μ, a shifting of the specular peak of 2 to about 10 deg occurred.

Such shifts have been noticed previously for CO_2 cryodeposits (Ref. 3). In addition, the occurrence of off-specular peaks at high incidence angles has been reported by several investigators (notably, Torrance and Sparrow, Ref. 8) for mechanically roughened surfaces. In the present tests the amount of the specular shift was essentially the same for the two larger deposit formation rates (Fig. 18), but a much smaller and relatively constant shift was indicated at the lowest formation rate. The amount of the specular shift for $\psi = 70$ deg is also shown for the largest formation rate (leak 1) but on paint coating 2. It is seen that the two different substrate coatings produced about the same value of $\Delta\theta$. Consequently, it is believed that large differences in $\Delta\theta$ between leaks 1 and 2 and leak 3 are not

caused by any alteration of the substrate. All of these facts do not yet allow a complete explanation of the cause of the off-specular peaks for cryodeposits on a black painted substrate. However, they do show that the shift of the off-specular peak depends on the frost formation rate, which in turn suggests that perhaps a much smoother deposit is formed at low formation rates. In any event, these off-specular peaks deserve further study.

5.5 SCATTERING INTERFERENCE PATTERNS

Interference patterns were also observed for the thin layers on a polished copper substrate (see Figs. 6 and 8). These patterns were not produced by Bragg refraction-reflection interference mentioned previously but were caused by interference of (1) rays reflected and scattered from the cryodeposit surface with (2) transmitted scattered rays. This scattering interference phenomenon is of some interest and can be utilized to measure the cryodeposit thickness and other properties of the cryodeposit. It is analyzed and discussed in Ref. 7. It is apparent from the logarithmic scale employed in Fig. 8 that the energy in these interference peaks is unimportant in comparison to that in the specular peak and that they are probably unimportant in thermal-vacuum testing. However, their existence together with the other factors described above serves to clearly illustrate that the reflection process for cryodeposits is extremely complex.

As explained in Ref. 7, these scattering interference patterns depend, in part, on strong specular reflections of scattered rays from the substrate. As a consequence, they will not be significant with a black substrate.

5.6 EFFECT OF DIFFUSION PUMP OIL CONTAMINATION

Most space simulation chambers also employ oil diffusion pumps, and the possibility of contaminating optical surfaces and/or the cryogenically cooled walls through backstreaming is ever present. Light distributions reflected from room temperature surfaces covered with thin films of diffusion pump oil are given in Ref. 9. If pump oil is present and the surfaces are cooled with LN_2, the oil forms a frost layer. The effects of a frost sublayer of pump oil on the reflective properties of CO_2 cryodeposits were determined, at least in a cursory way, during this investigation.

A small but unmeasured quantity of pump oil was introduced into the chamber which formed a film on the polished copper surface. When the surface was cooled to 77°K, a thin oil cryodeposit formed. It reflected light in a highly specular manner, but at all angles of incidence the amount of reflected radiant energy at the specular angle was reduced by 10 percent from the values previously measured for a clean copper surface (Fig. 12). Then CO_2 was allowed to flow into the chamber, and cryodeposits of various thicknesses were formed. A few comparisons of the normalized distributions of reflected light measured with and without an oil frost sublayer are given in Fig. 19. In all cases the data were normalized by the reference values for a clean copper surface (Fig. 12). Consequently, a 10-percent reduction of the level of the distributions for the oil-contaminated surface would be expected. Figure 19 indicates that the distributions measured with an oil sublayer were similar to those obtained with the surface clean but that the contaminated surface generally reflected much less light than expected. This was particularly true for the thinner layers. Comparisons at other deposit thicknesses or angles of incidence yielded the same results as shown in Fig. 19.

SECTION VI
CONCLUSIONS

Measurement of the angular distribution of light reflected from CO_2 cryodeposits having thicknesses from 1 to 270 μ and formed on polished copper and black epoxy painted substrates has lead to the following conclusions:

1. Carbon dioxide cryodeposits have a diffusing effect on light at wavelengths from about 0.4 to 1.2 μ. Specularly reflected light from the substrate diminishes with increasing cryodeposit thickness. The specular component of the reflected light disappears completely at deposit thicknesses between about 60 and 100 μ.
2. Carbon dioxide cryodeposits with thicknesses over about 100 μ reflect light essentially diffusely.
3. For very thin layers (below 2 μ) the amount of light reflected from cryodeposits is significantly influenced by Bragg interference.

4. The amount of specularly reflected light from both polished copper and black substrates may be significantly reduced by forming cryodeposits on the surface with thicknesses below about 100 μ.

5. At thicknesses over about 100 μ the amount of energy reflected from the deposit tends to increase with increasing cryodeposit thickness.

6. Strong backscattering along the incident beam, scattering interference peaks, and an angular shift of the specular peak were all observed. These and other factors mentioned above served to illustrate that the reflection of light from CO_2 cryodeposits is a complex phenomenon.

In regard to the complication introduced in thermal-vacuum space simulation tests by cryodeposits forming on the cold chamber walls, the investigation reported herein indicates the following:

1. If the cryodeposits are very thin (less than 2 μ or 0.002 mm), reflections from the cryogenically cooled chamber walls are greatly complicated by Bragg interference phenomena. Wall corrections to thermal balance test data will be extremely difficult to derive and apply. However, in most cases these corrections would be very small and probably negligible.

2. If the cryodeposit thickness is between 2 to 70 μ (0.002 and 0.07 mm), wall corrections will have to include terms for specularly reflected light. Also, cryodeposits in this range may be useful in decreasing the amount of light reflected from the chamber walls.

3. When the cryodeposit thickness is greater than about 100 μ (0.1 mm), wall corrections to thermal balance test data become increasingly more important. Fortunately, the wall may be treated as a diffuse reflector, which should significantly simplify the determination of thermal balance correction factors.

REFERENCES

1. Cunningham, T. M., Jr. and Young, R. L. "The Radiative Properties of Carbon Dioxide Cryodeposits at 77°K." AEDC-TDR-62-165 (AD291165), December 1962.

2. Cunningham, T. M., Jr. and Young, R. L. "The Absorptance of a Water Cryodeposit at 77°K for 350°K Radiation." AEDC-TDR-63-155 (AD414429), August 1963.

3. McCullough, B. A., Wood, B. E., and Dawson, J. P. "Thermal Radiative Properties of Carbon Dioxide Cryodeposits from 0.5 to 1.1 microns." AEDC-TR-65-94 (AD468632), August 1965.

4. Wood, B. E., McCullough, B. A., Dawson, J. P., and Birkebak, R. C. "Vacuum Integrating Spheres for Measuring Cryodeposit Reflectances from 0.35 to 15 microns." AEDC-TR-65-178 (AD468608), August 1965.

5. McCullough, B. A., Wood, B. E., and Smith, A. M. "A Vacuum Integrating Sphere for In Situ Reflectance Measurements at 77°K from 0.5 to 10 microns." AEDC-TR-67-10 (AD650072), April 1967.

6. Wood, B. E., Smith, A. M., and McCullough, B. A. "The Spectral Reflectance of Water and Carbon Dioxide Cryodeposits from 0.36 to 1.15 microns." AEDC-TR-67-131 (AD657018), May 1967.

7. Tempelmeyer, K. E., Wood, B. E., and Mills, D. W., Jr. "In Situ Measurement of Thickness and Other Properties of Carbon Dioxide Cryodeposits by Optical Techniques." AEDC-TR-67-226 (AD662869), December 1967.

8. Torrance, K. E. and Sparrow, E. M. "Off-Specular Peaks in the Directional Distribution of Reflected Thermal Radiation." ASME Paper No. 65-WA/HT-19, December 1965.

9. Pinion, C. E. "Effects of Diffusion Pump Oil Contamination on the Reflectance Characteristics of Various Surfaces." AEDC-TR-66-53 (AD635897), July 1966.

APPENDIX
ILLUSTRATIONS

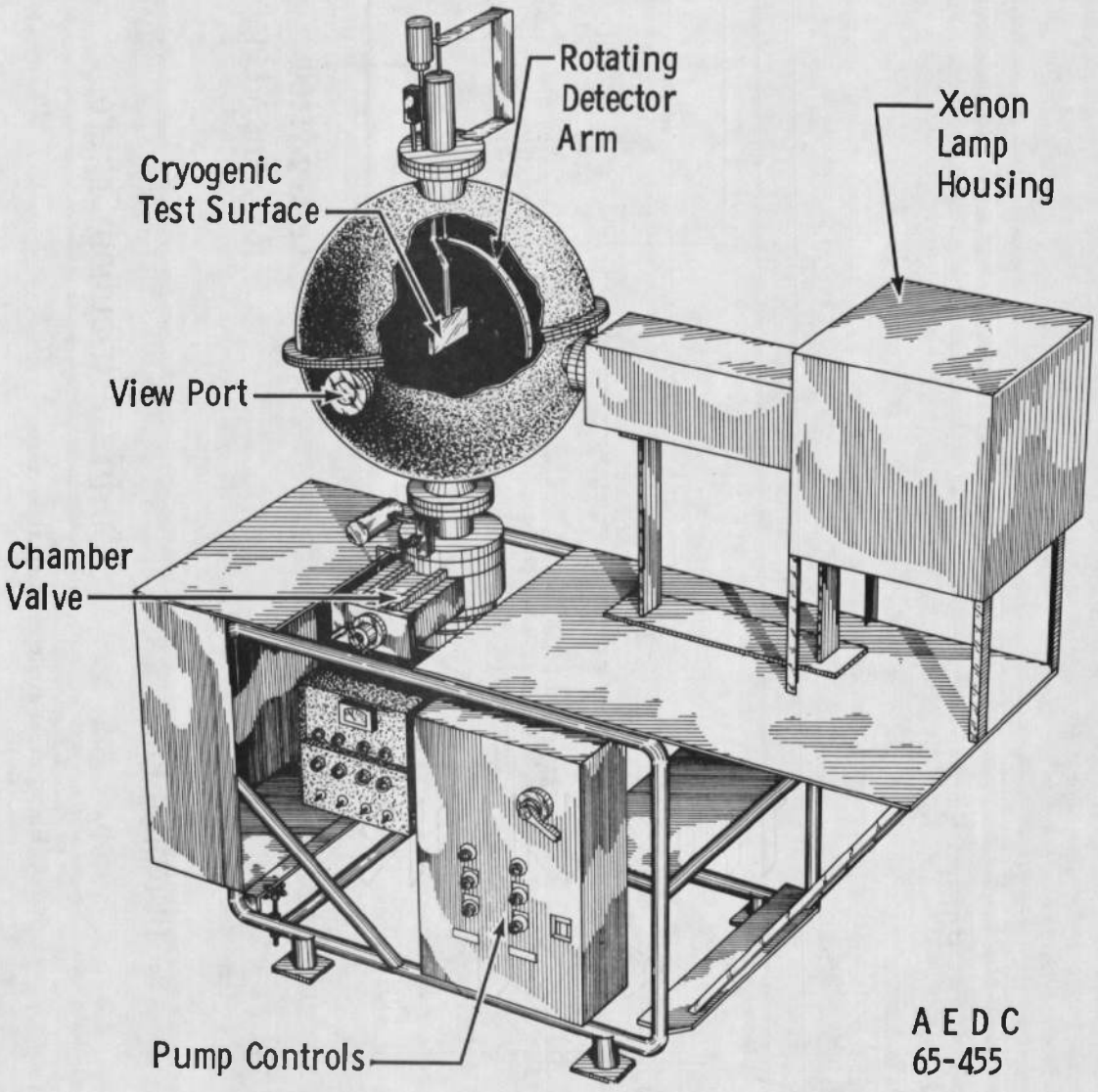

Fig. 1 Schematic of Test Apparatus

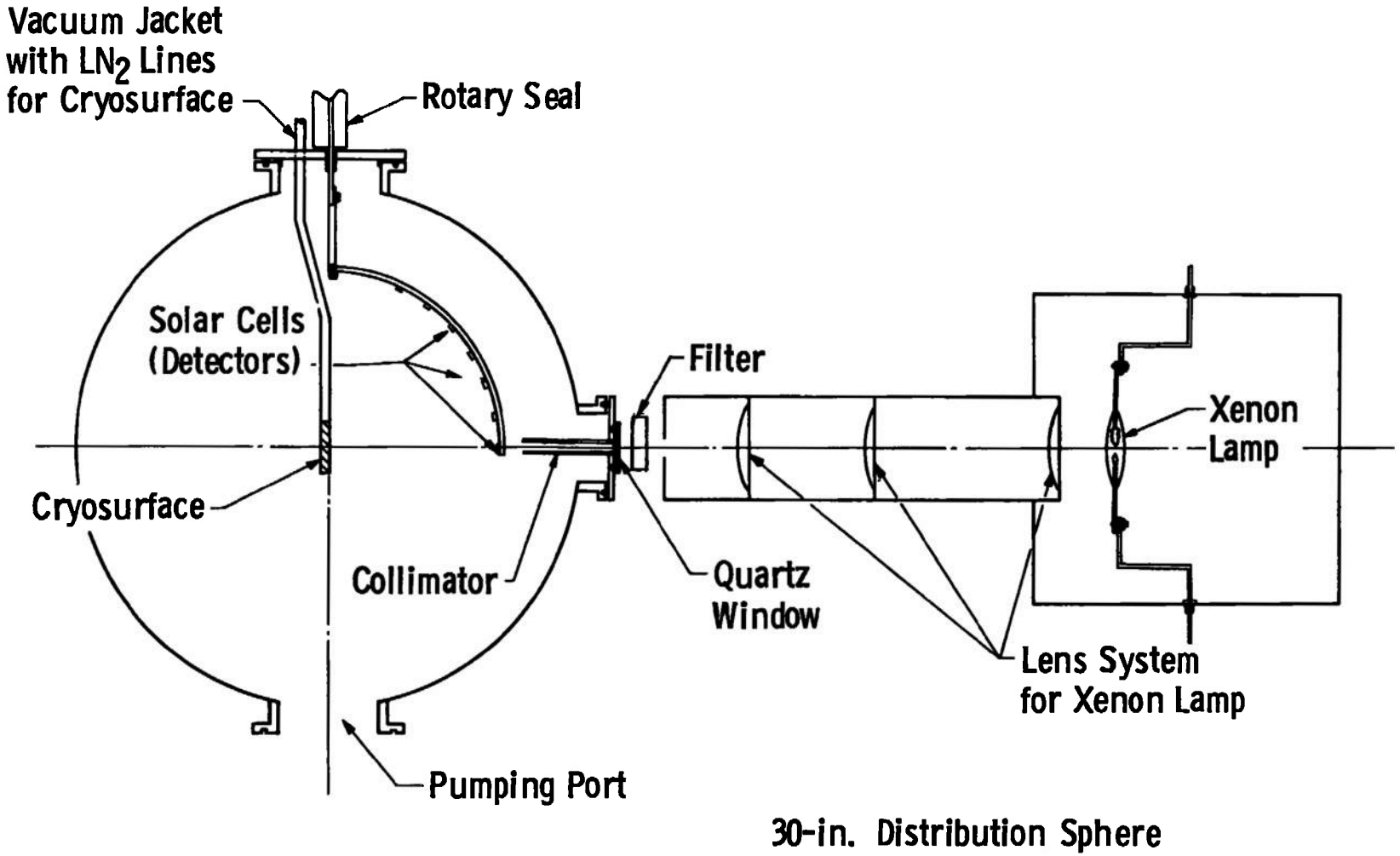

Fig. 2 Schematic of Optical System

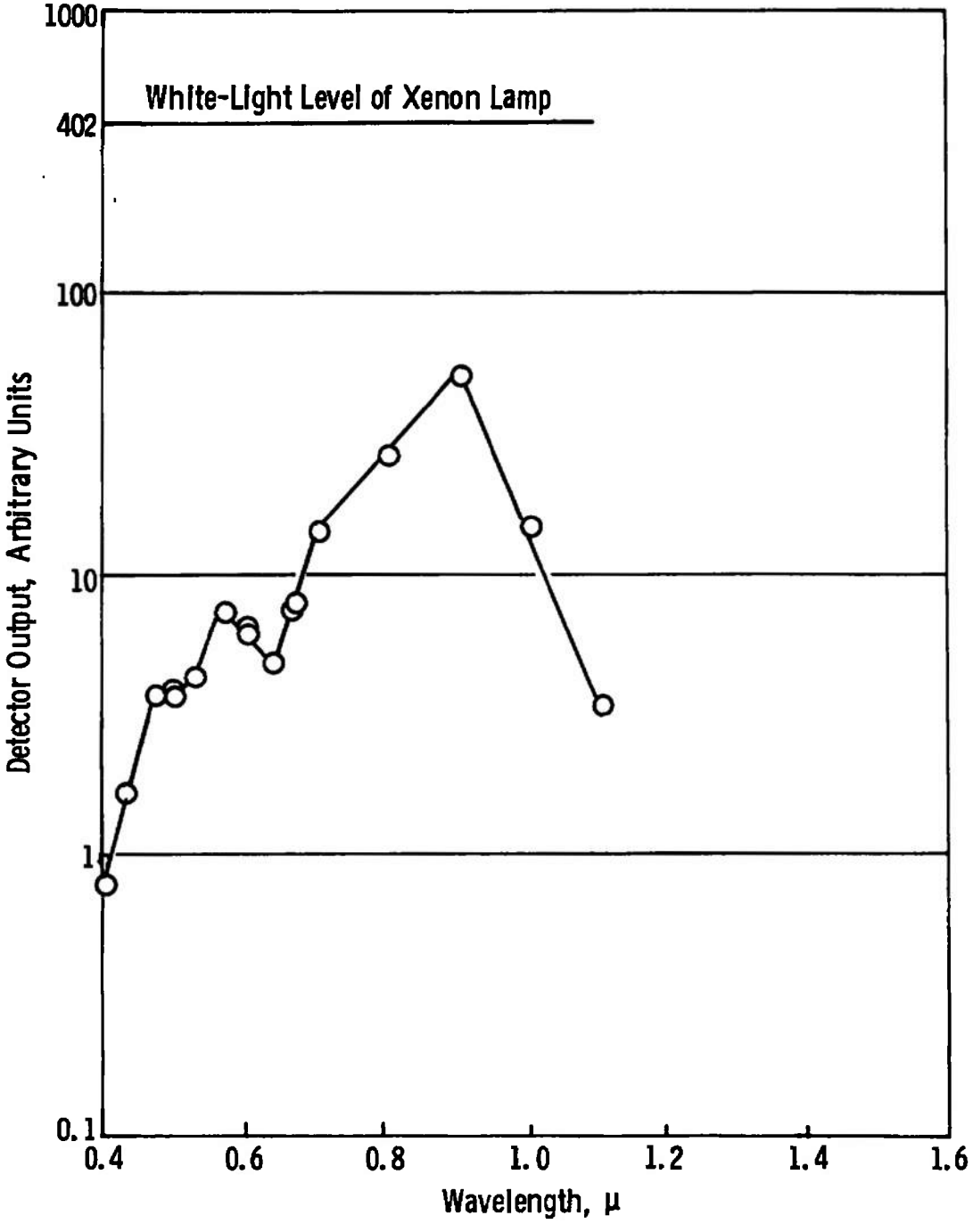

Fig. 3 Composite Spectrum of the Light Source and Detector Systems

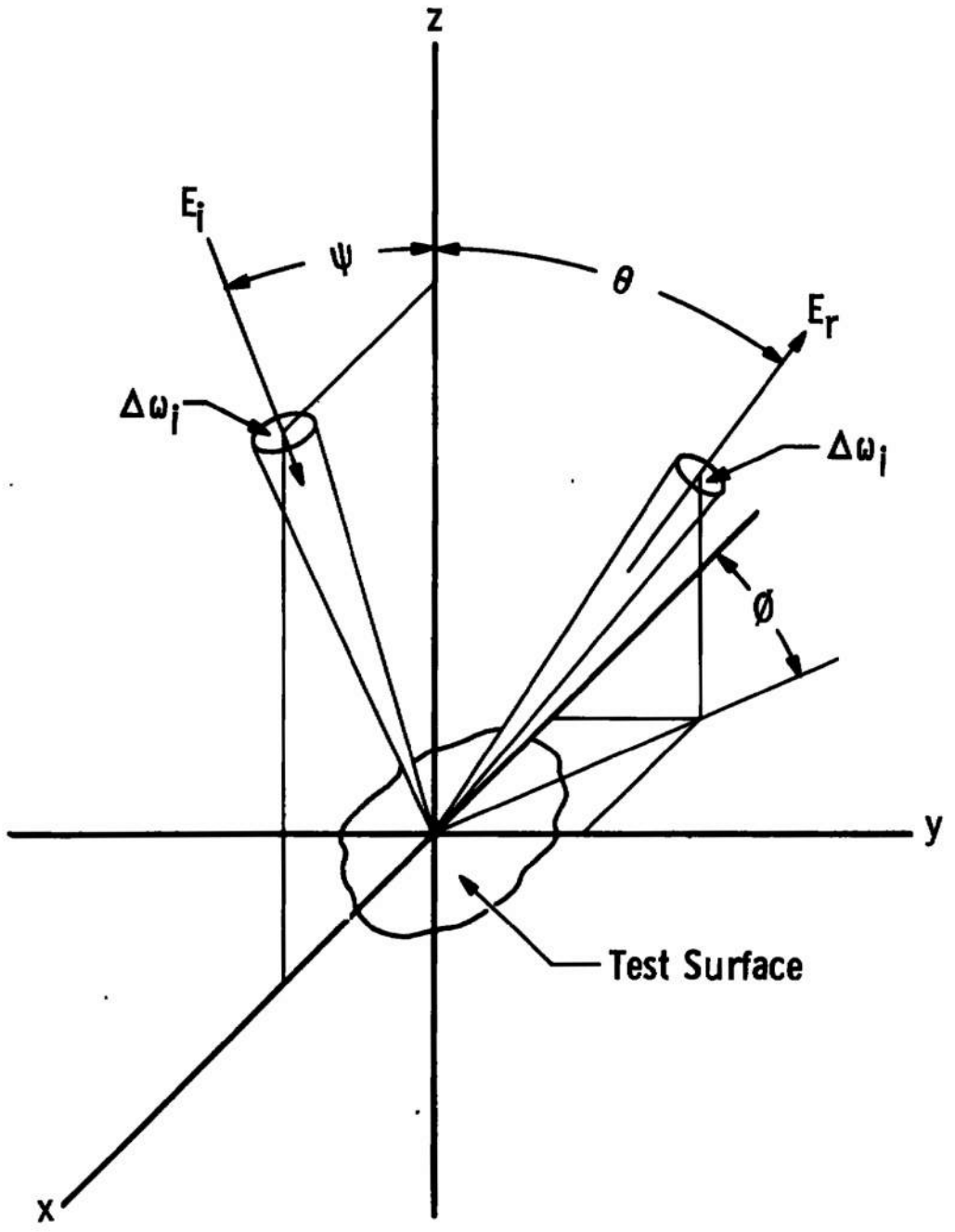

Fig. 4 Notation Pertinent to Biangular Distribution Measurements

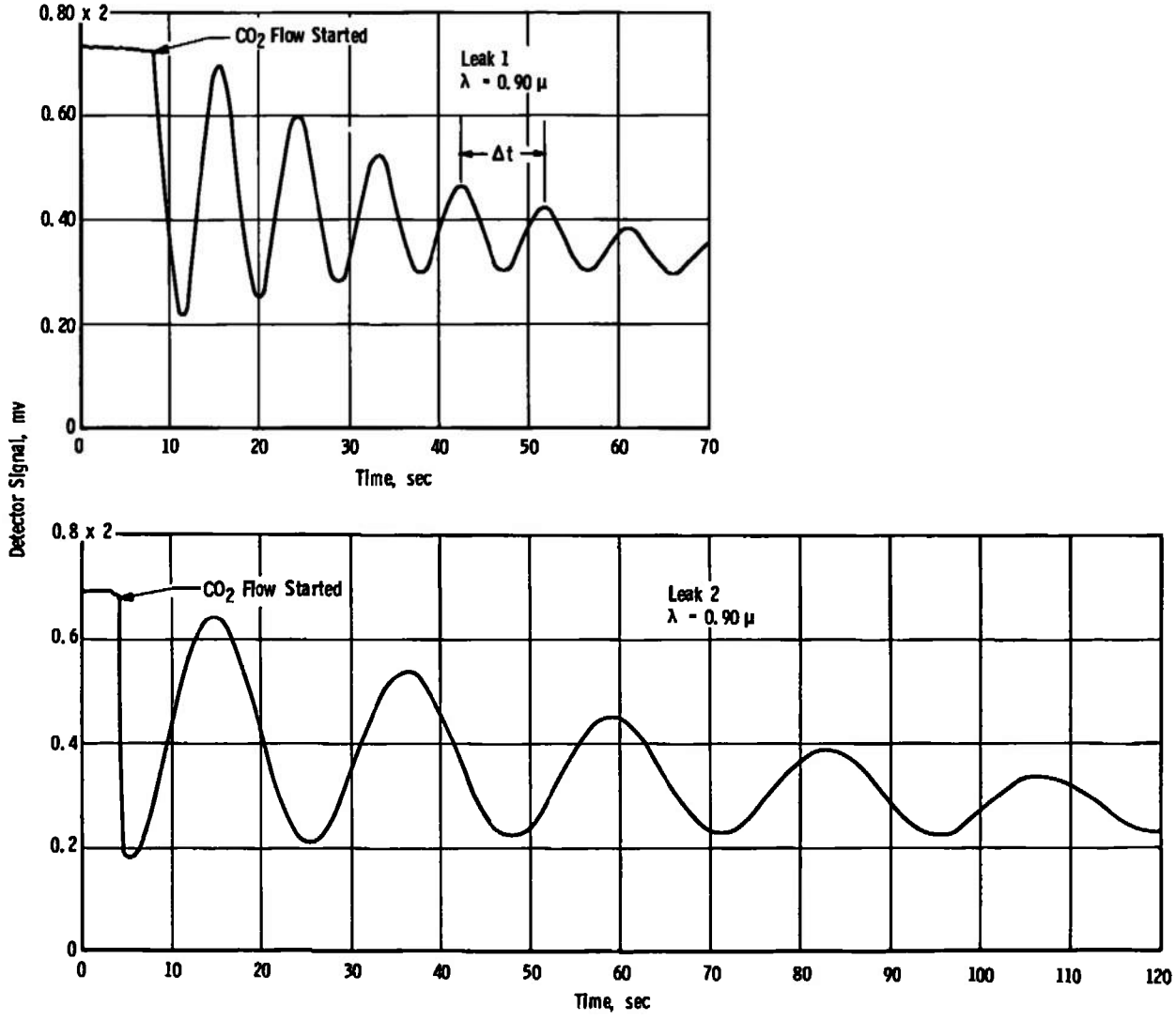

Fig. 5 Typical Bragg Interference Patterns for a Black Substrate

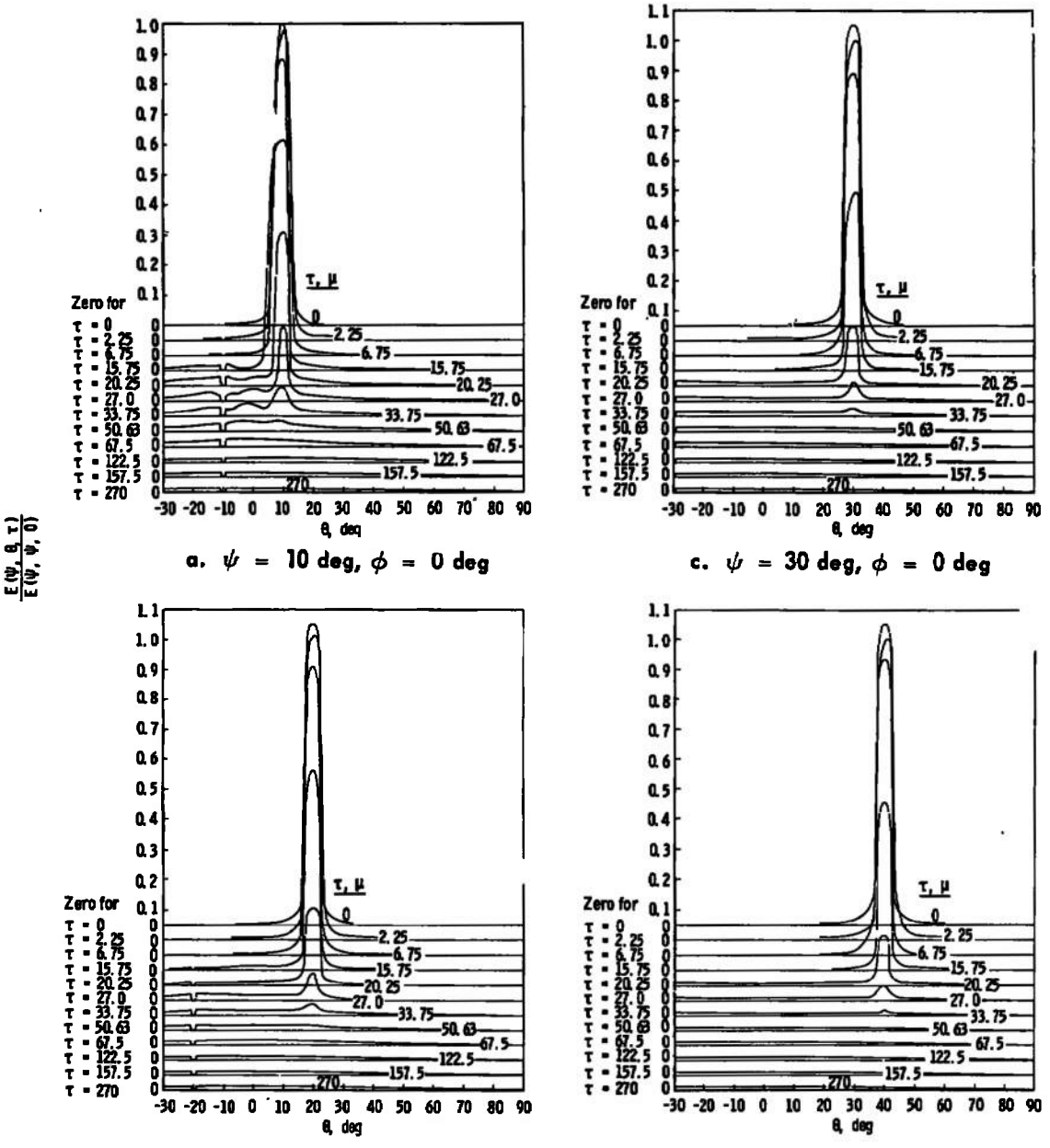

Fig. 6 Normalized Distribution of Light Reflected from CO_2 Cryodeposits Formed at Various Thicknesses on a Polished Copper Substrate at a Rate of 2.25 μ/min

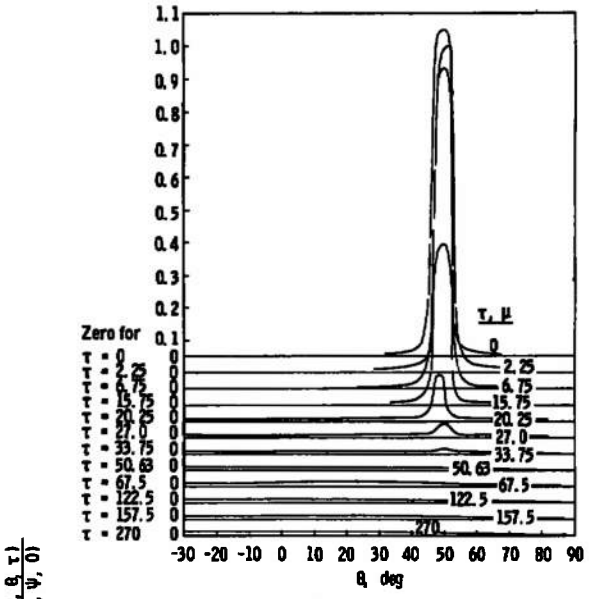

e. ψ = 50 deg, ϕ = 0 deg

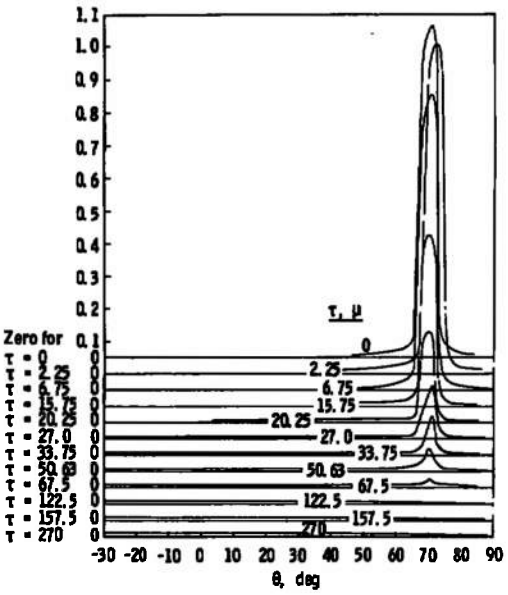

g. ψ = 70 deg, ϕ = 0 deg

$\frac{E(\Psi, \theta, \tau)}{E(\Psi, \Psi, 0)}$

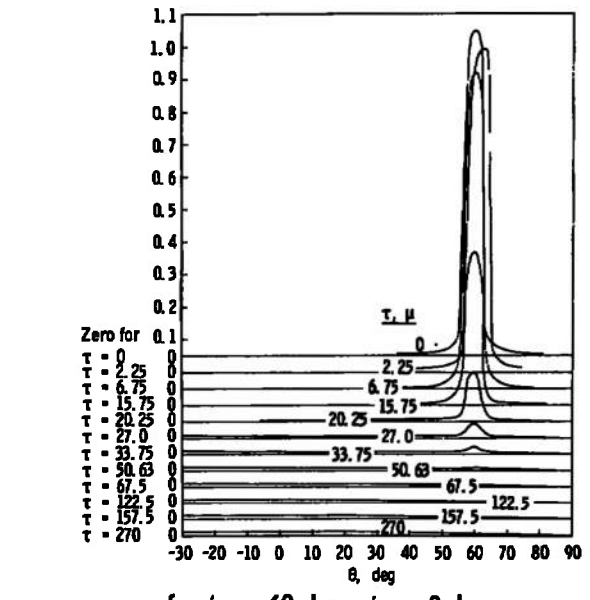

f. ψ = 60 deg, ϕ = 0 deg

Fig. 6 Concluded

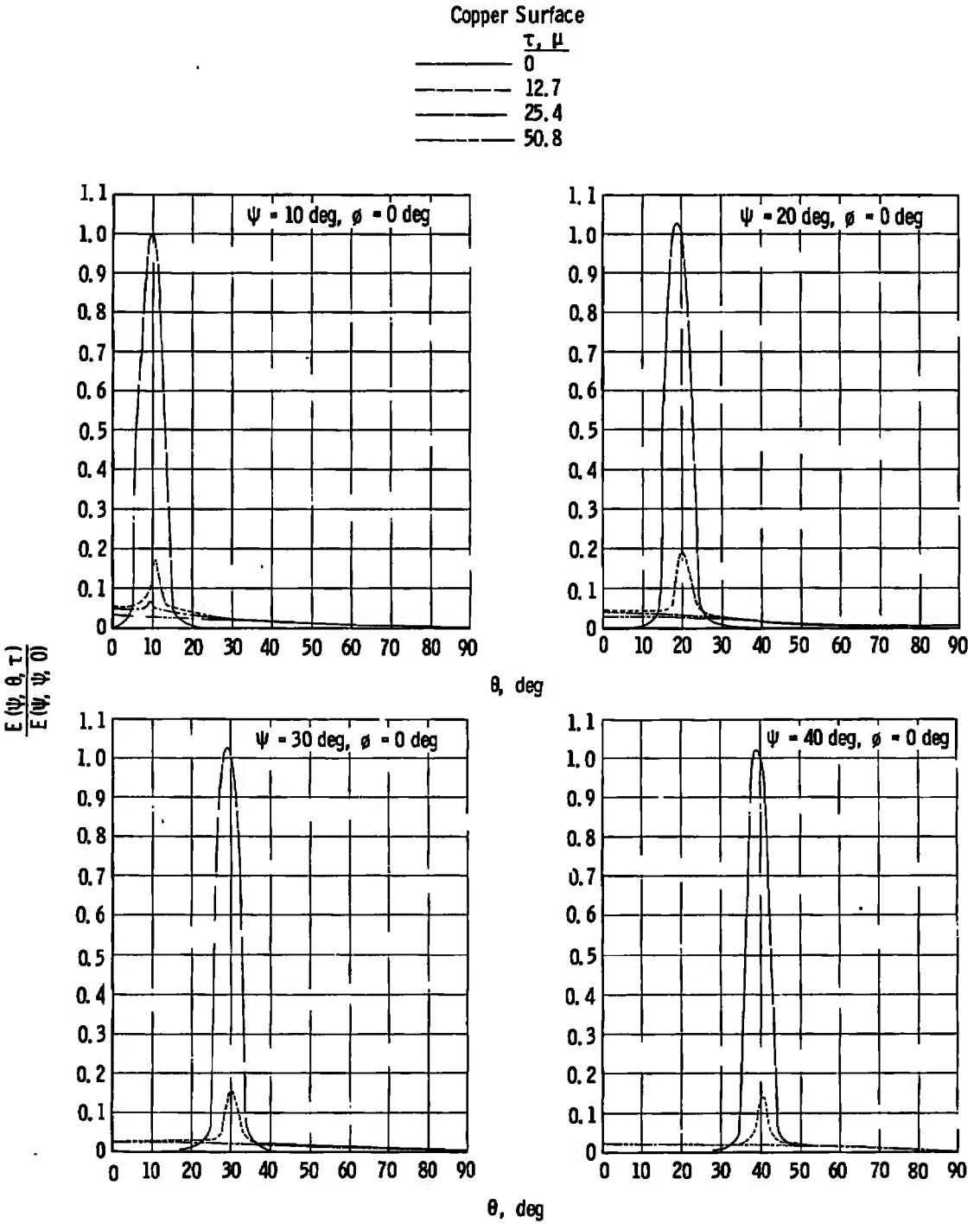

Fig. 7 Normalized Distribution of Light Reflected from CO_2 Cryodeposits Formed at Various Thicknesses on a Polished Copper Substrate at a Rate of 0.423 μ/min

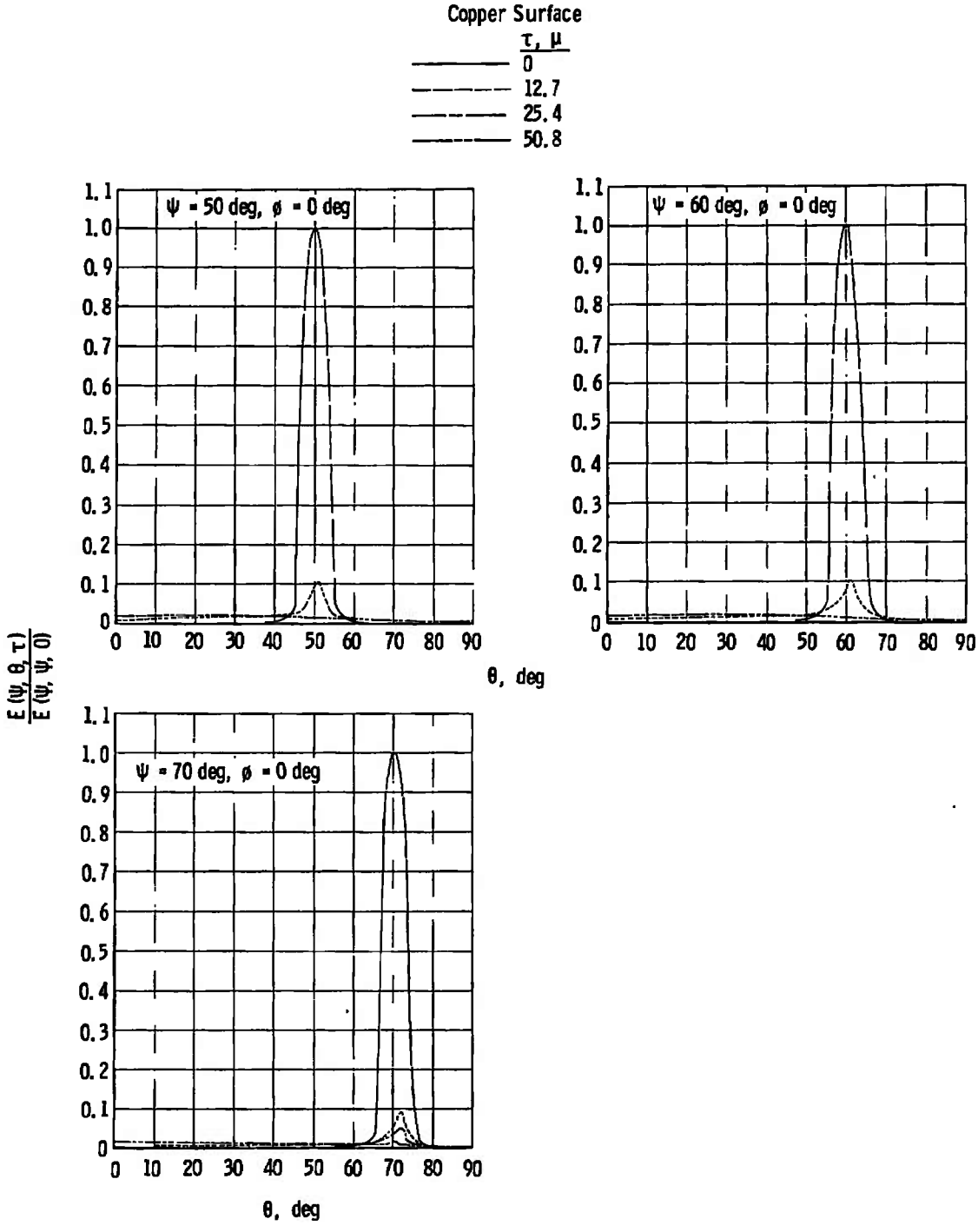

Fig. 7 Concluded

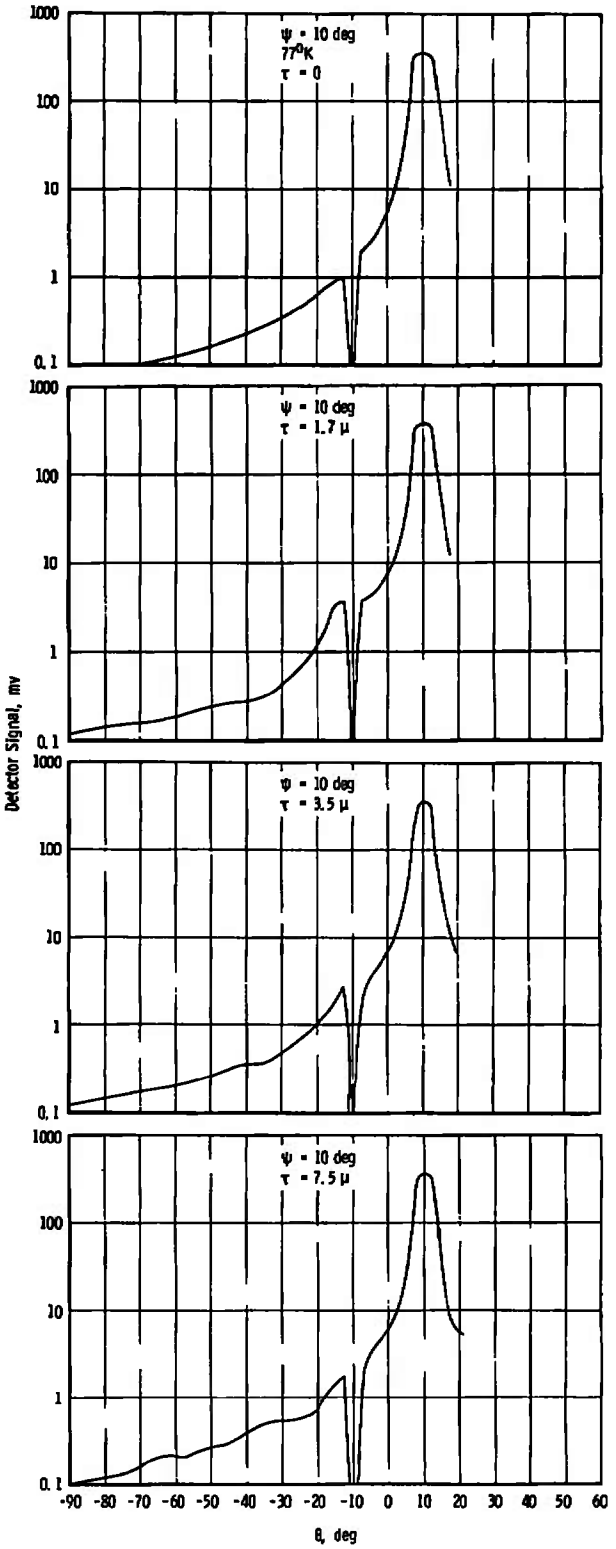

Fig. 8 Distribution of Light Reflected from CO_2 Cryodeposits Formed at Various Thicknesses on a Polished Copper Substrate at a Rate of 0.0385 μ/min and with ϕ = 0 deg

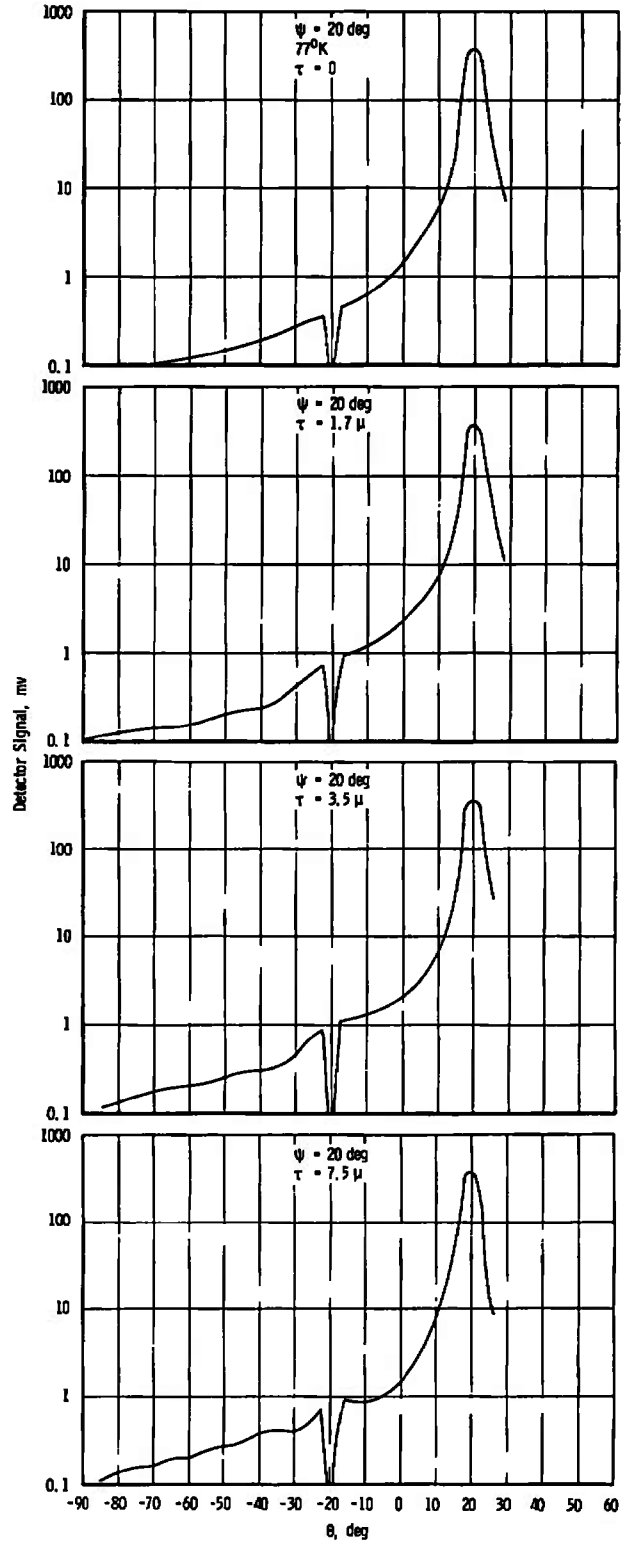

Fig. 8 Continued

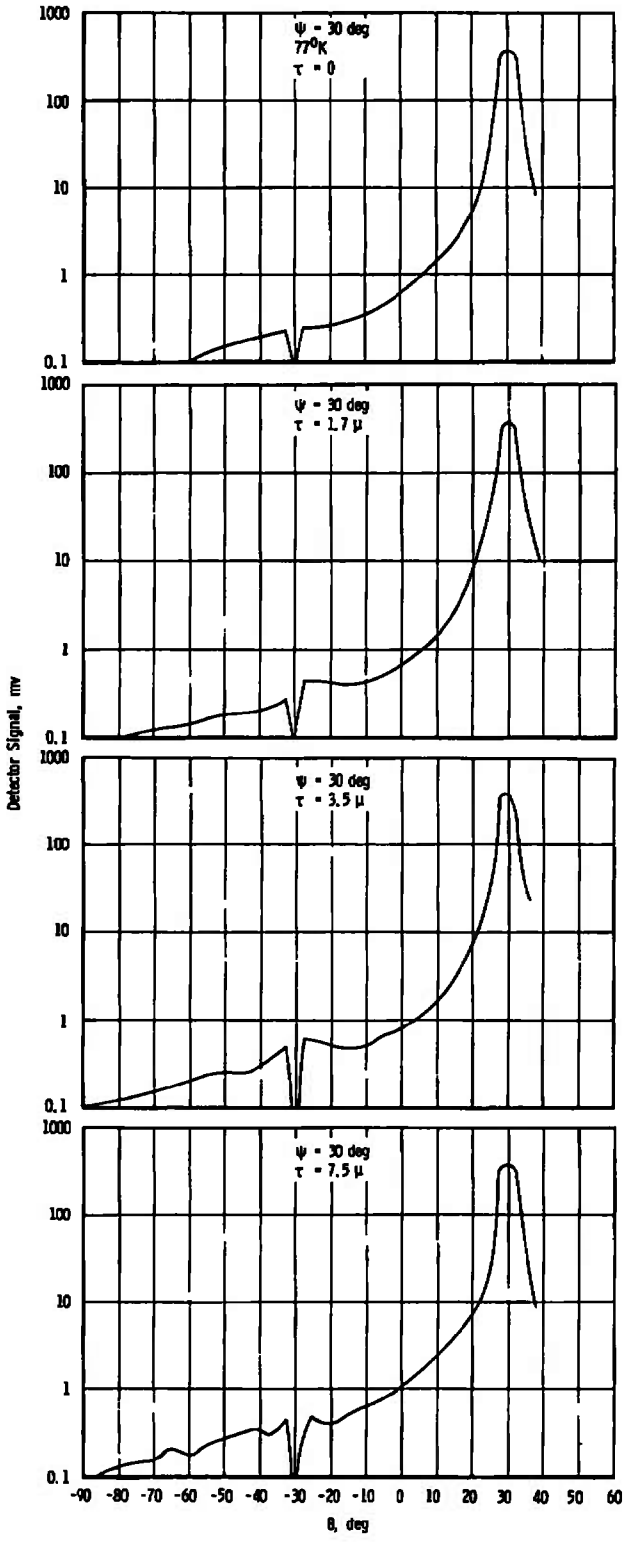

Fig. 8 Continued

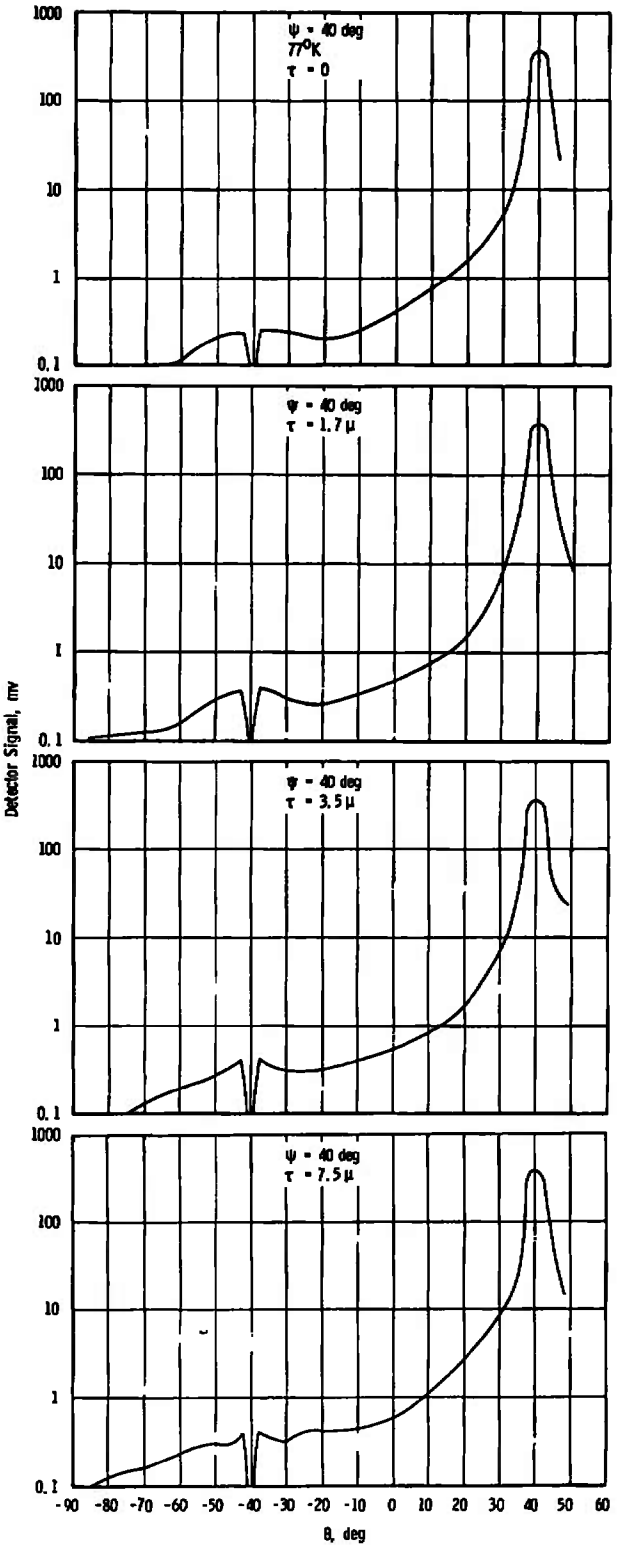

Fig. 8 Continued

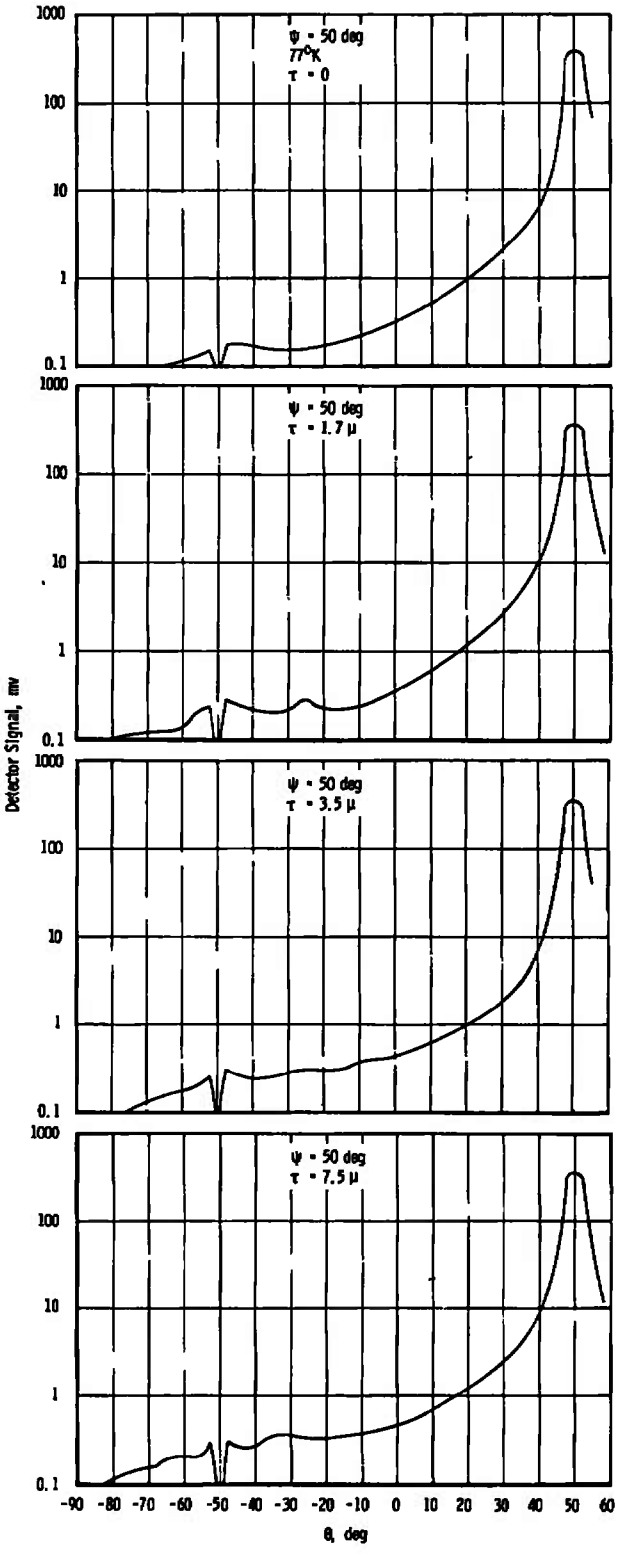

Fig. 8 Continued

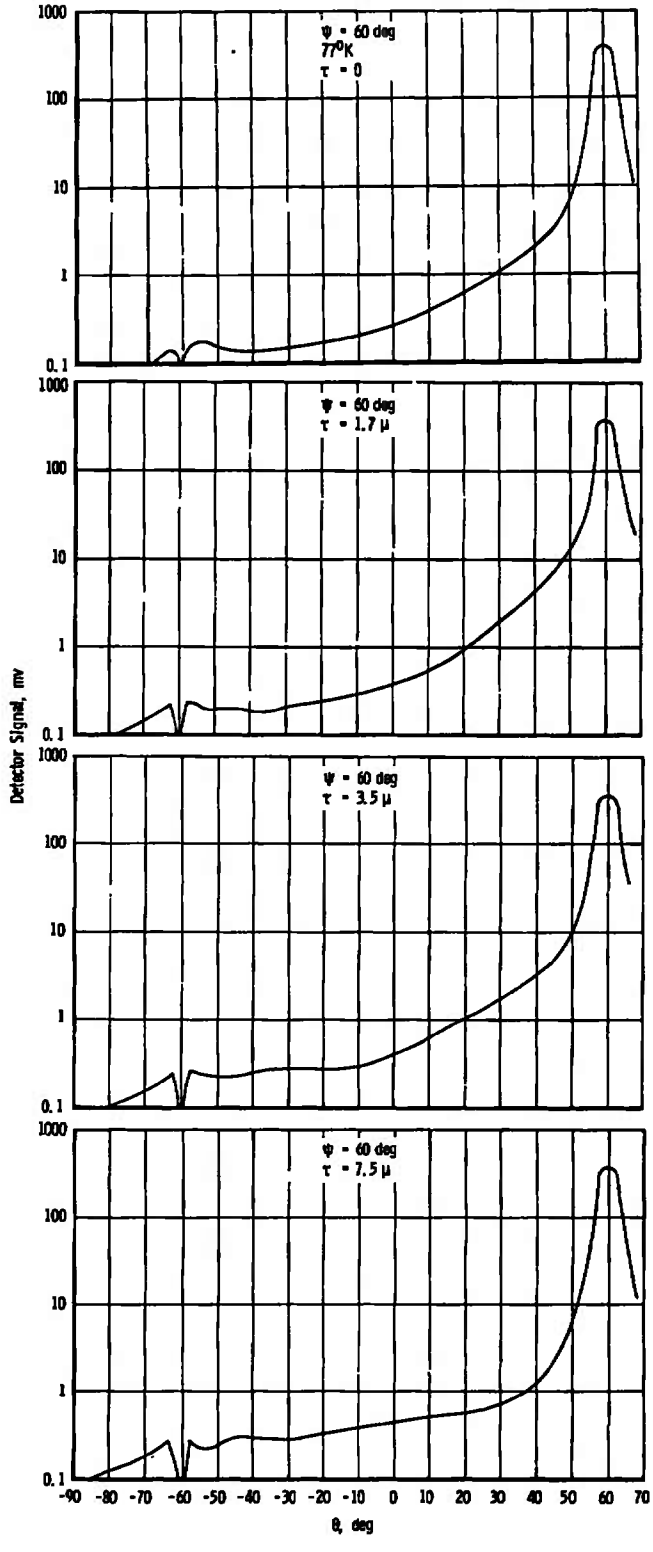

Fig. 8 Continued

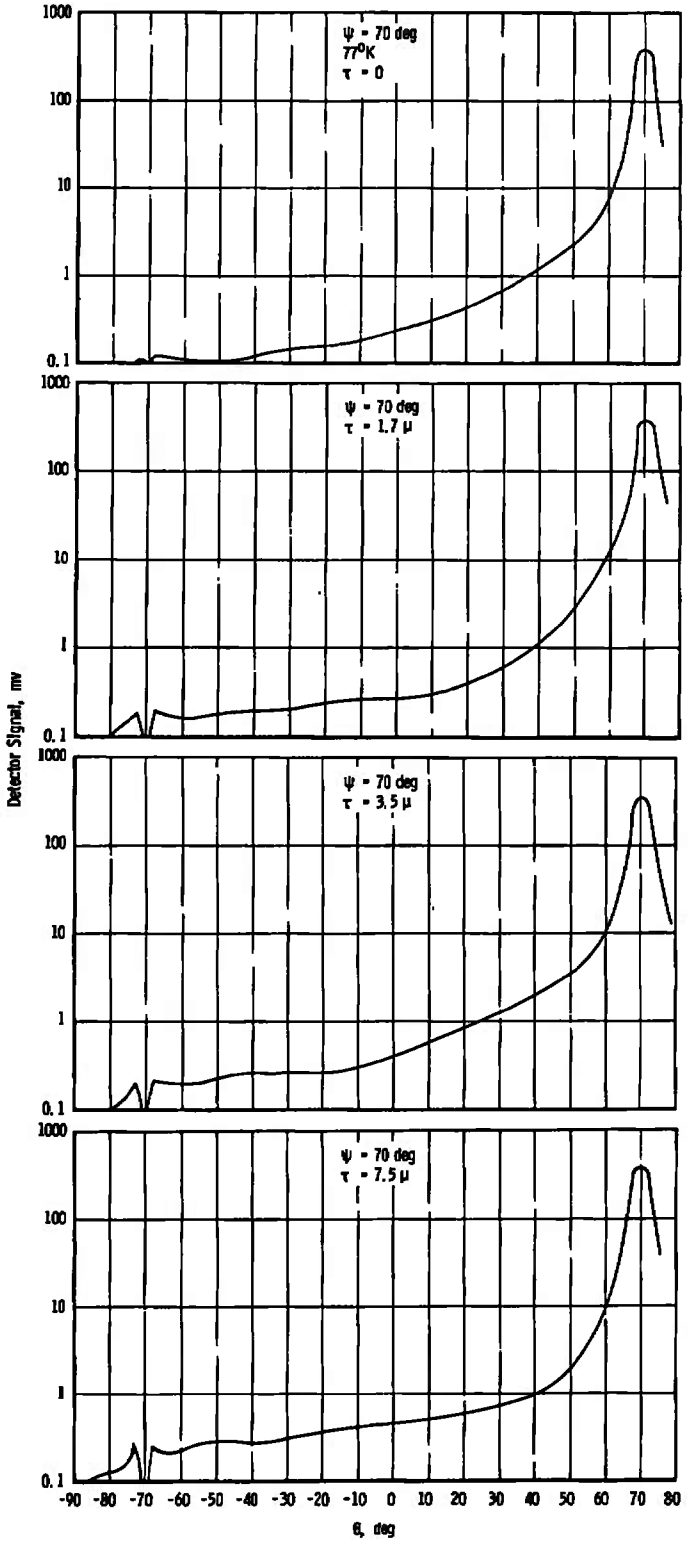

Fig. 8 Concluded

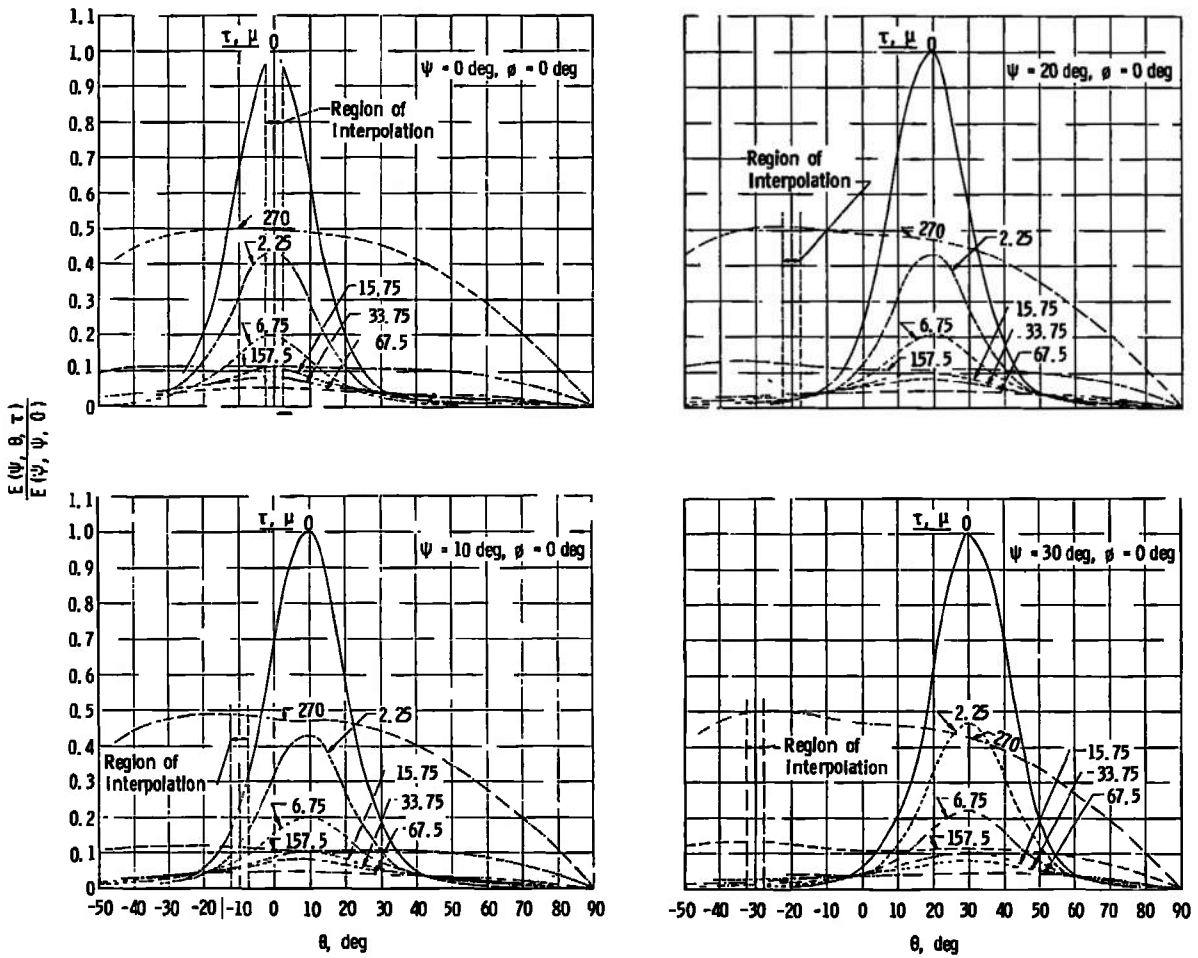

Fig. 9 Normalized Distribution of Light Reflected from CO_2 Cryodeposits Formed at Various Thicknesses on a Black Epoxy Painted Substrate at a Rate of 2.25 μ/min and with ϕ = 0 deg

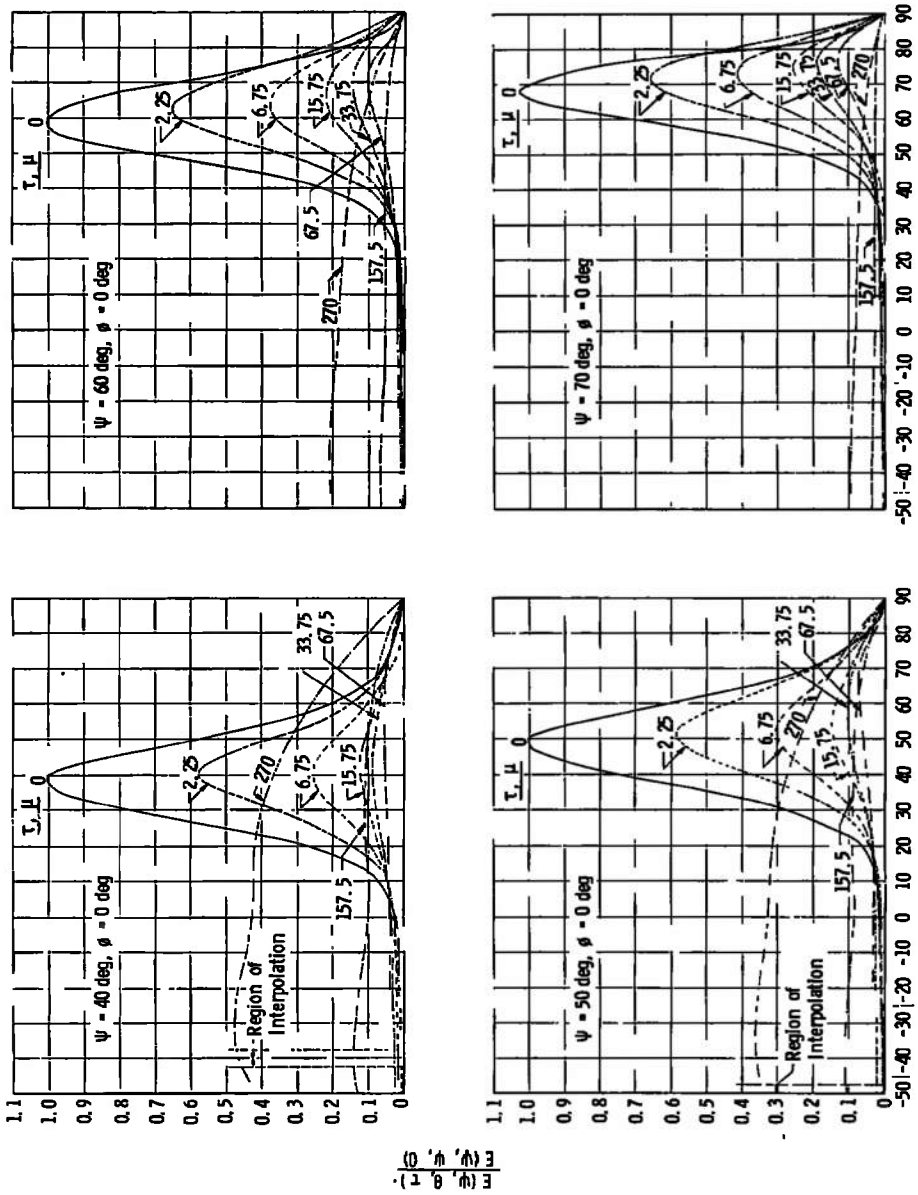

Fig. 9 Concluded

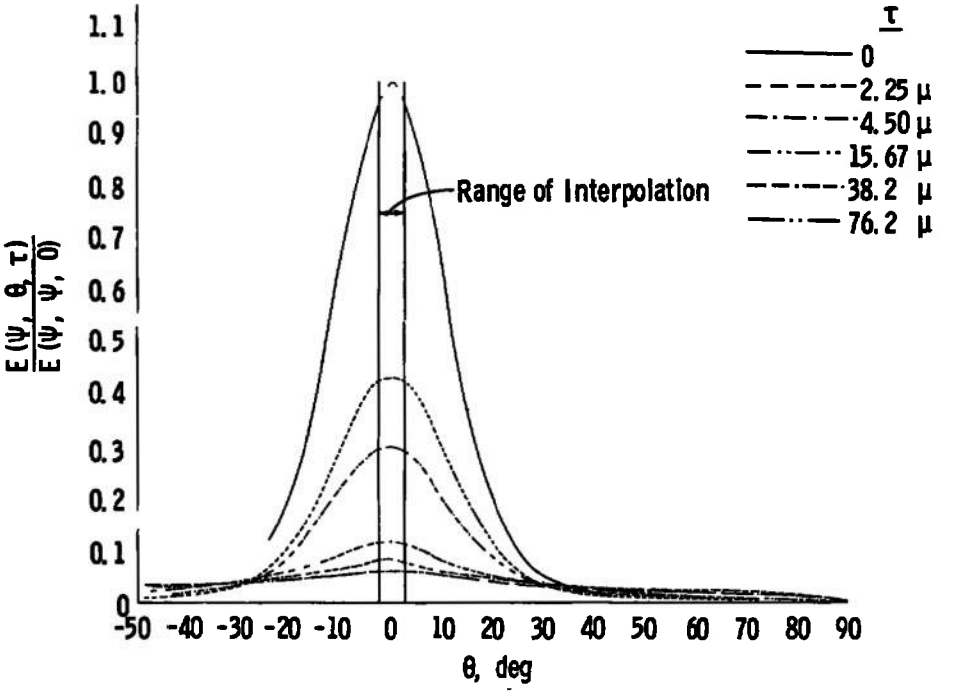

a. ψ = 0 deg

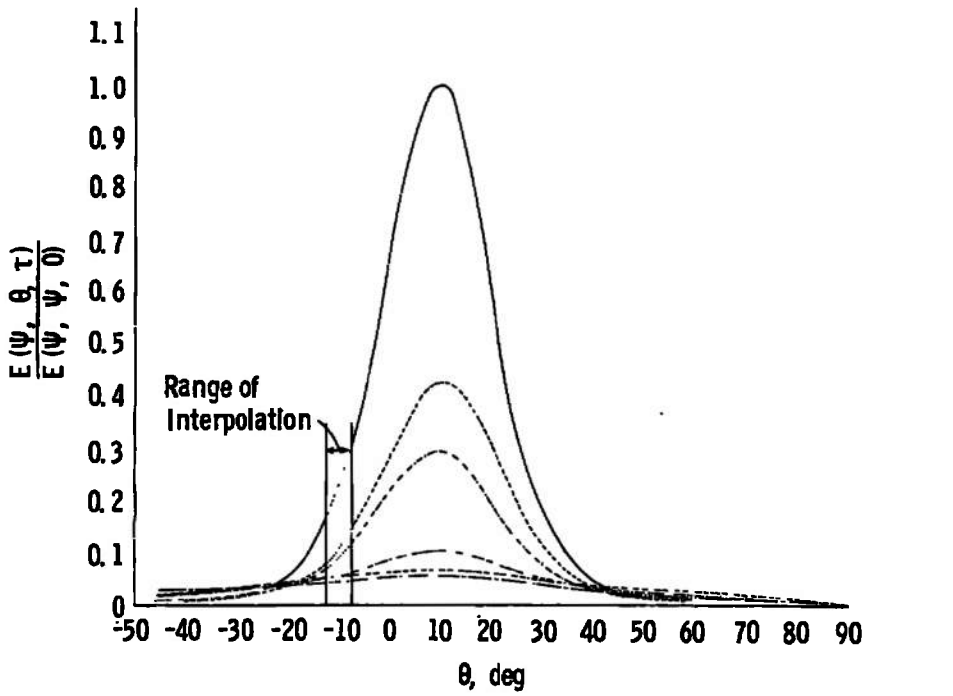

b. ψ = 10 deg

Fig. 10 Normalized Distribution of Light Reflected from CO_2 Cryodeposits Formed at Various Thicknesses on a Black Epoxy Painted Substrate at a Rate of 0.423 μ/min and with ϕ = 0 deg

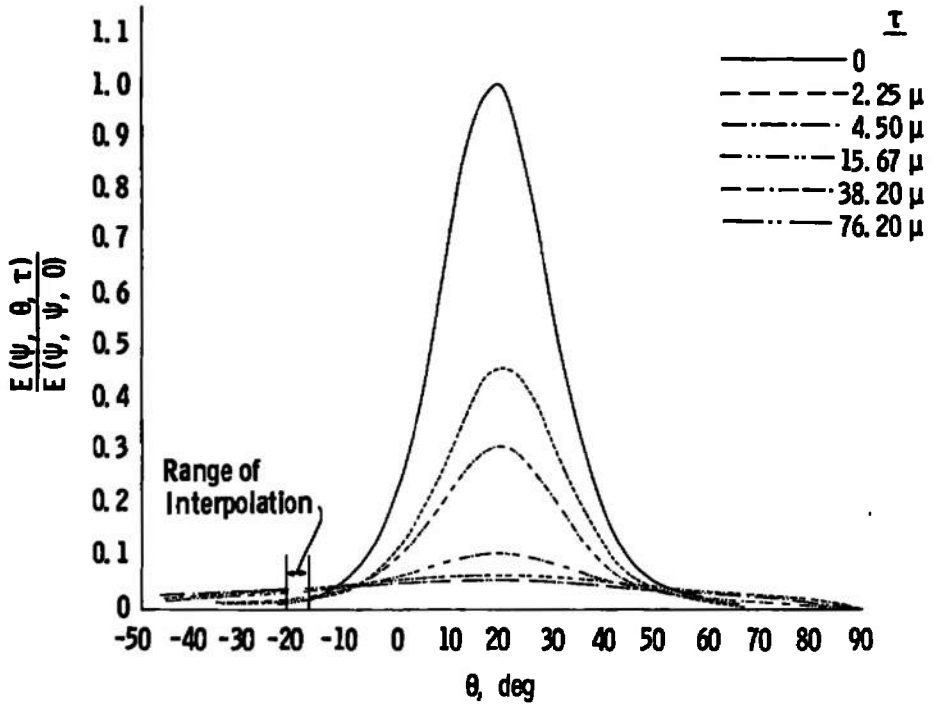

c. ψ = 20 deg

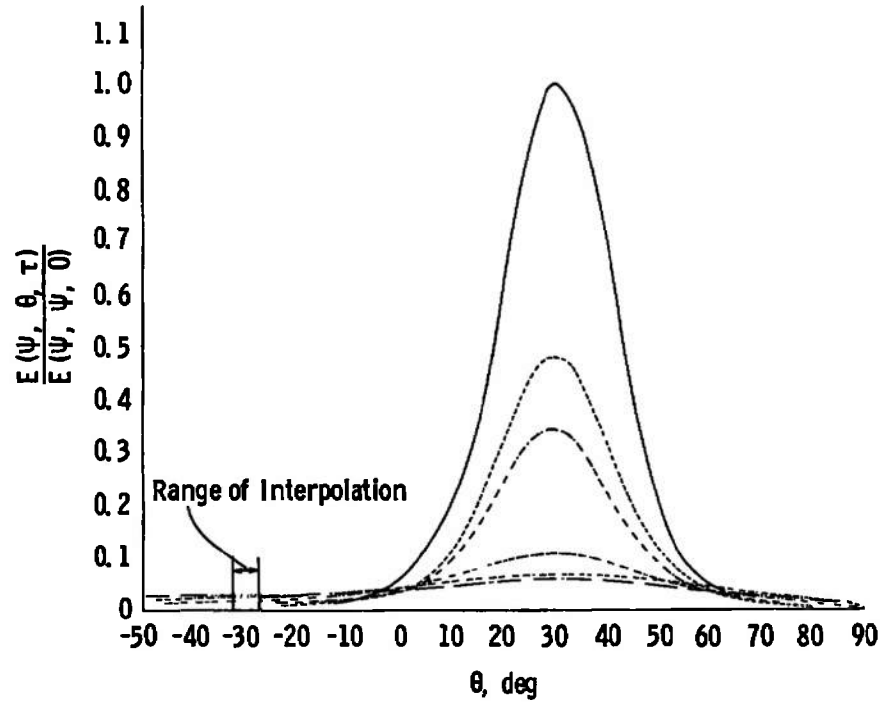

d. ψ = 30 deg

Fig. 10 Continued

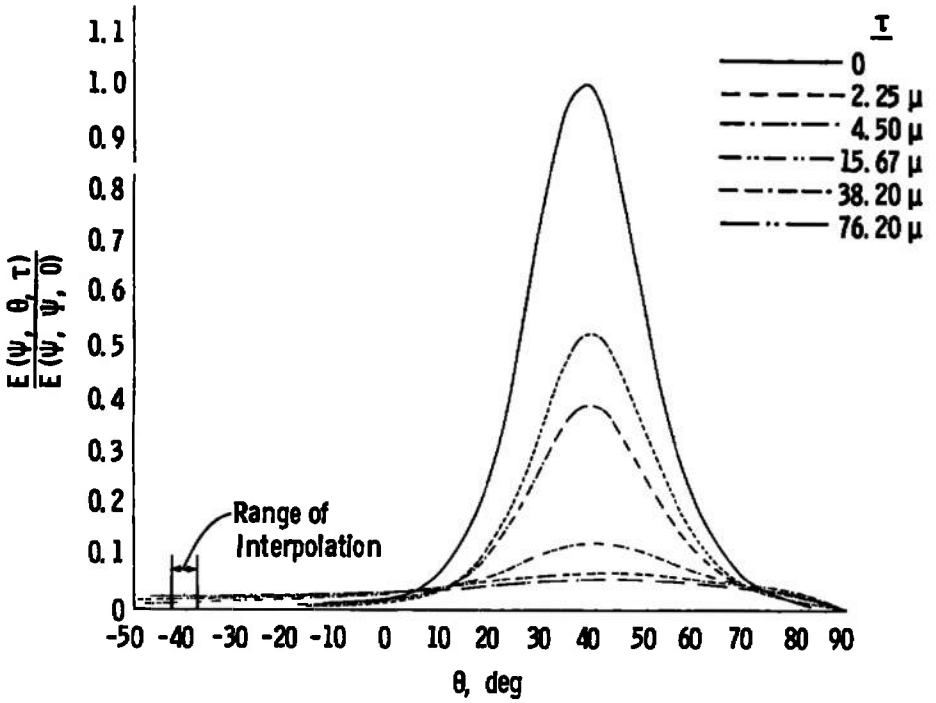

e. ψ = 40 deg

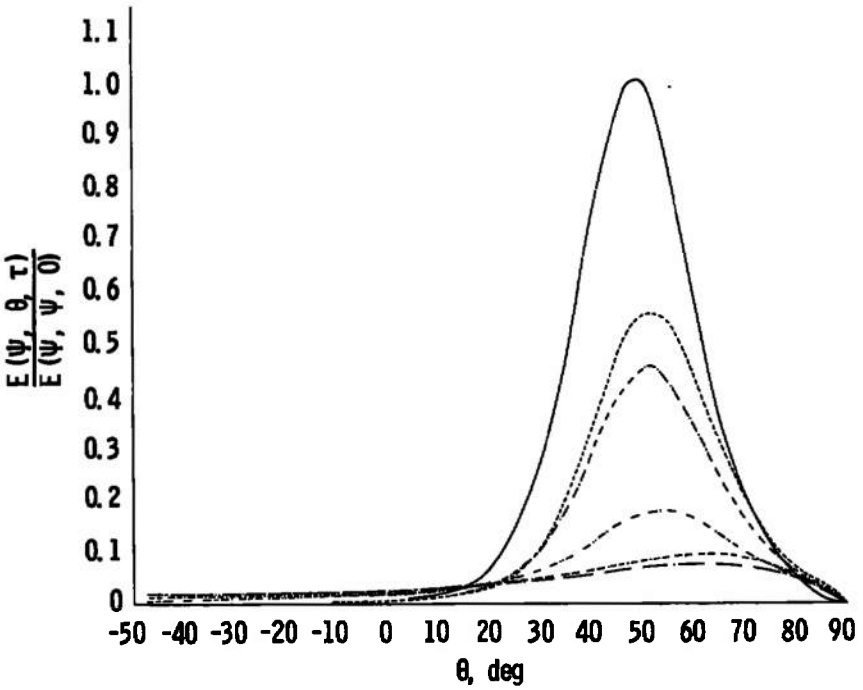

f. ψ = 50 deg

Fig. 10 Continued

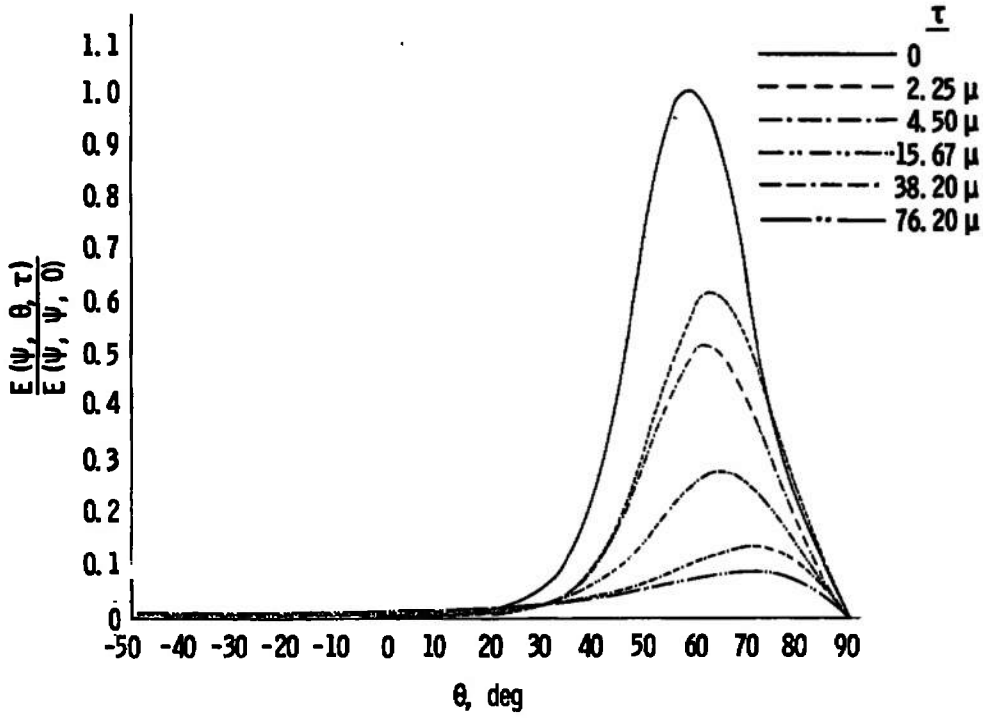

g. ψ = 60 deg

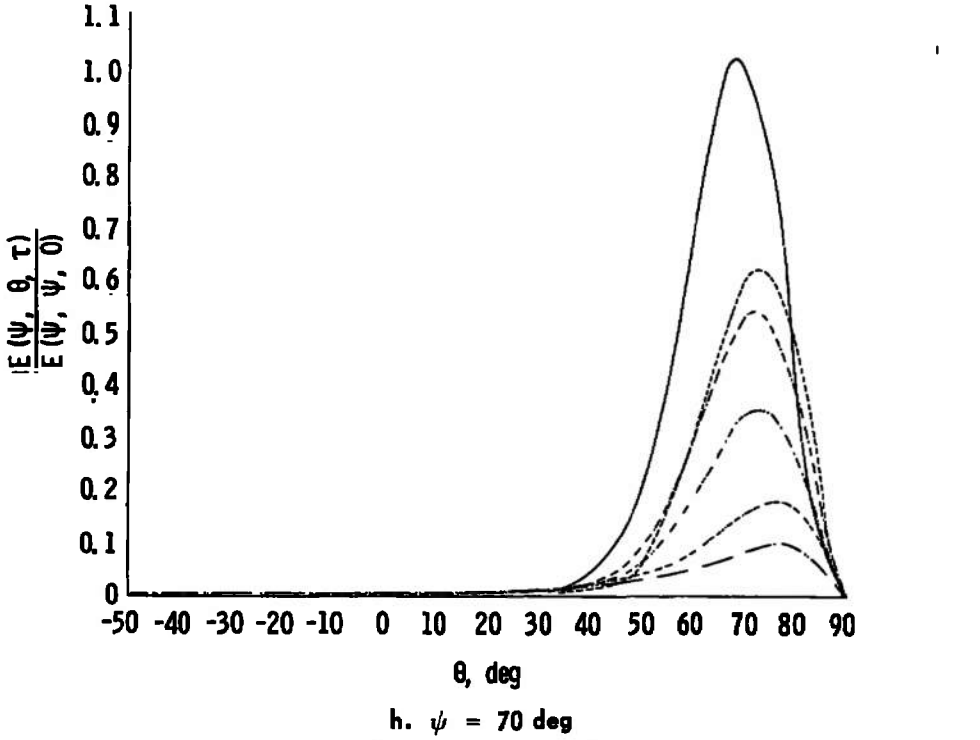

h. ψ = 70 deg

Fig. 10 Concluded

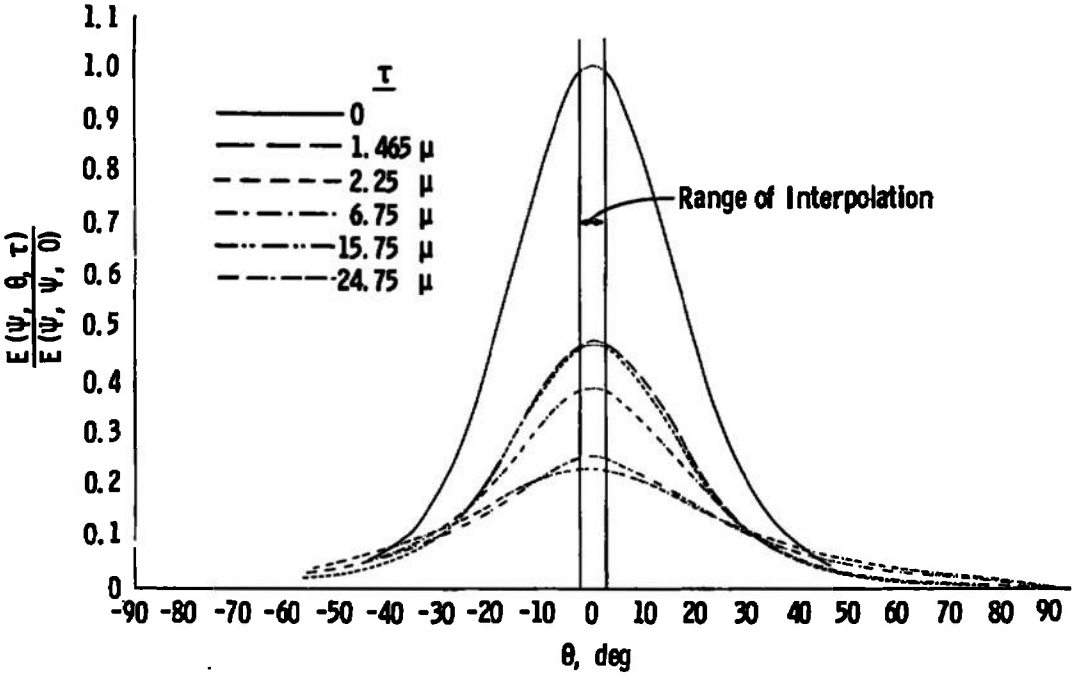

a. ψ = 0 deg

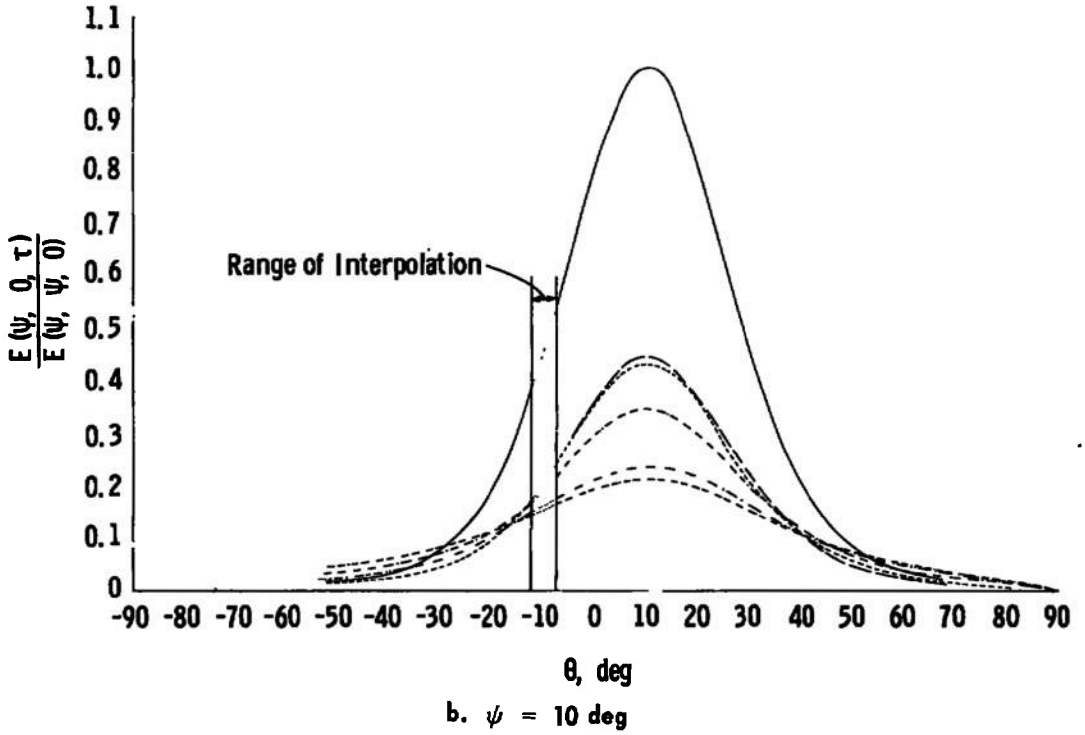

b. ψ = 10 deg

Fig. 11 Normalized Distribution of Light Reflected from CO_2 Cryodeposits Formed at Various Thicknesses on a Black Epoxy Painted Substrate at a Rate of 0.0385 μ/min and with ϕ = 0 deg

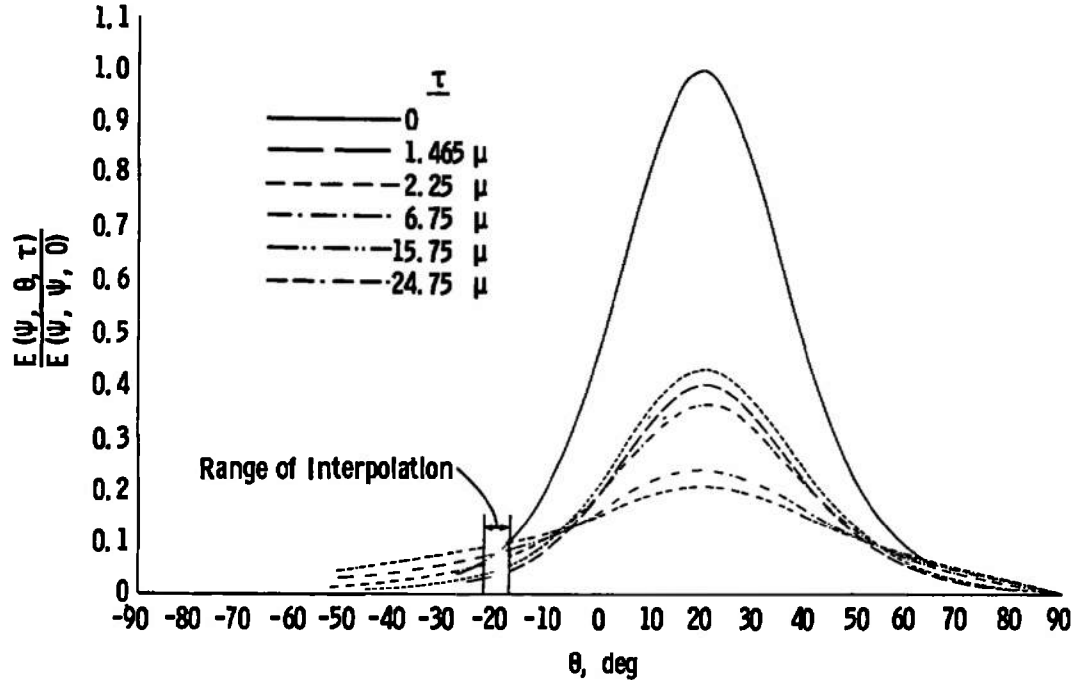

c. ψ = 20 deg

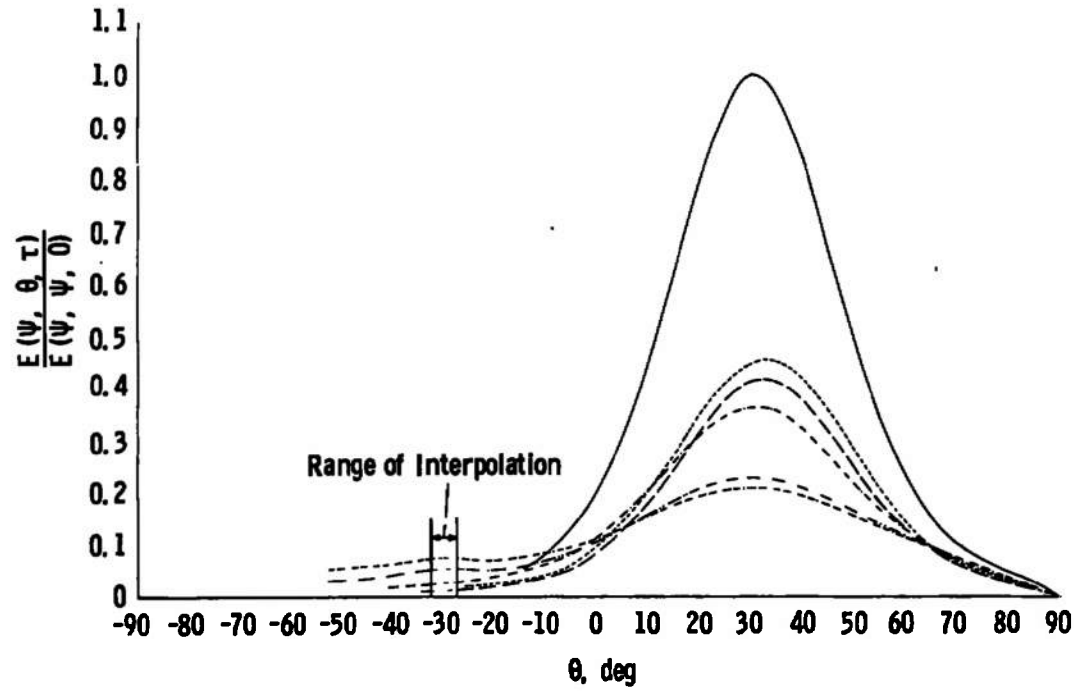

d. ψ = 30 deg

Fig. 11 Continued

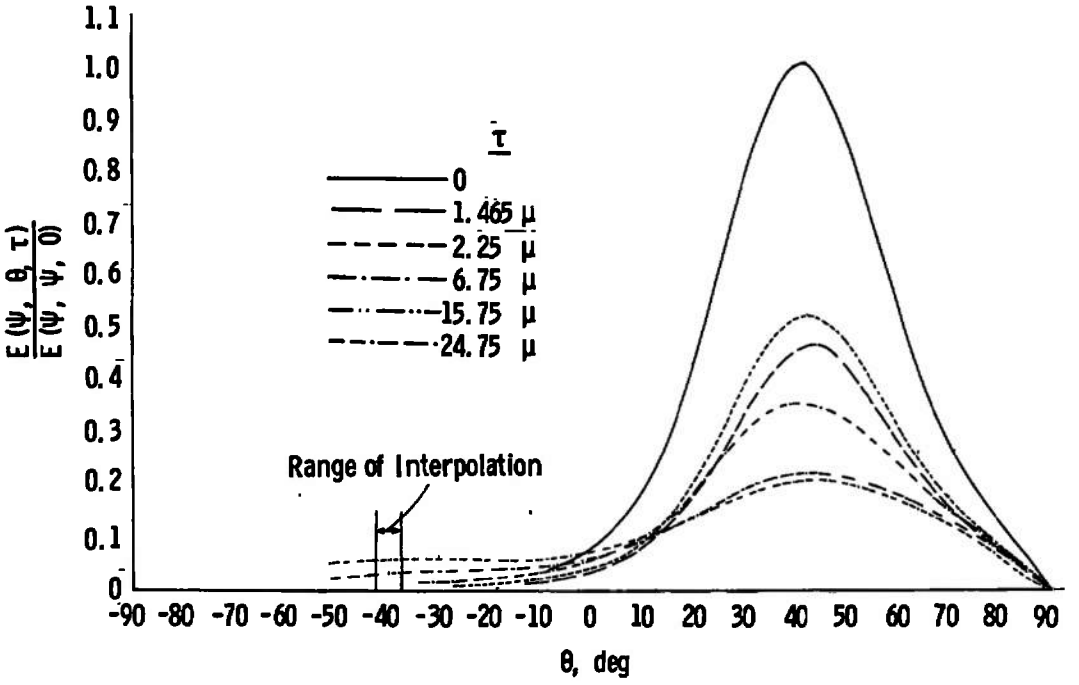

e. ψ = 40 deg

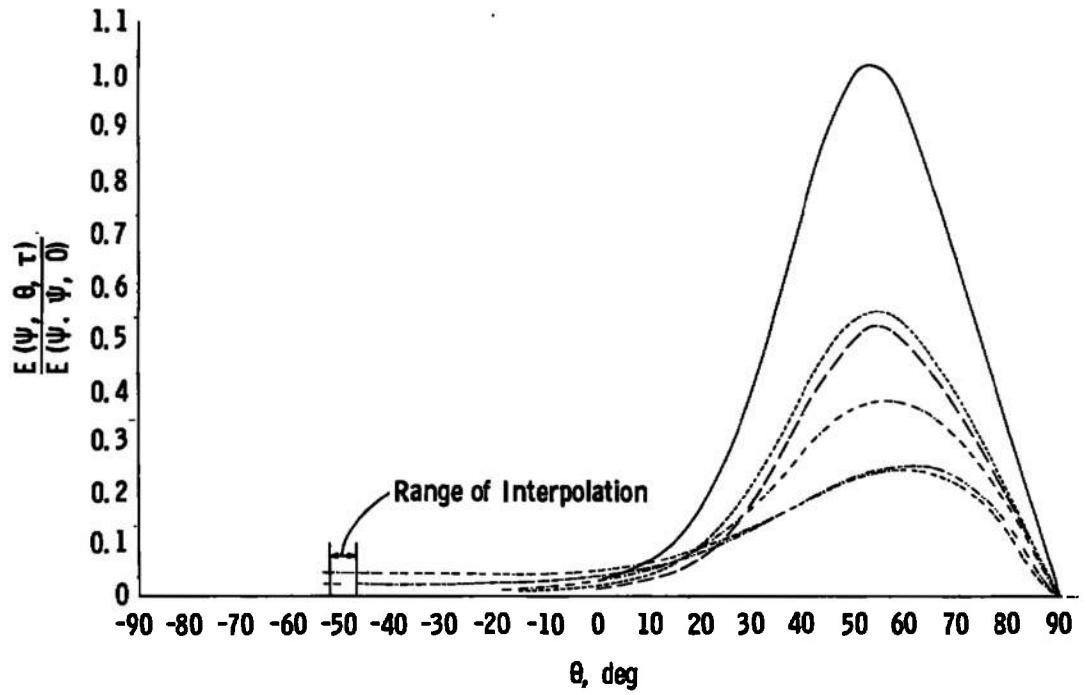

f. ψ = 50 deg

Fig. 11 Continued

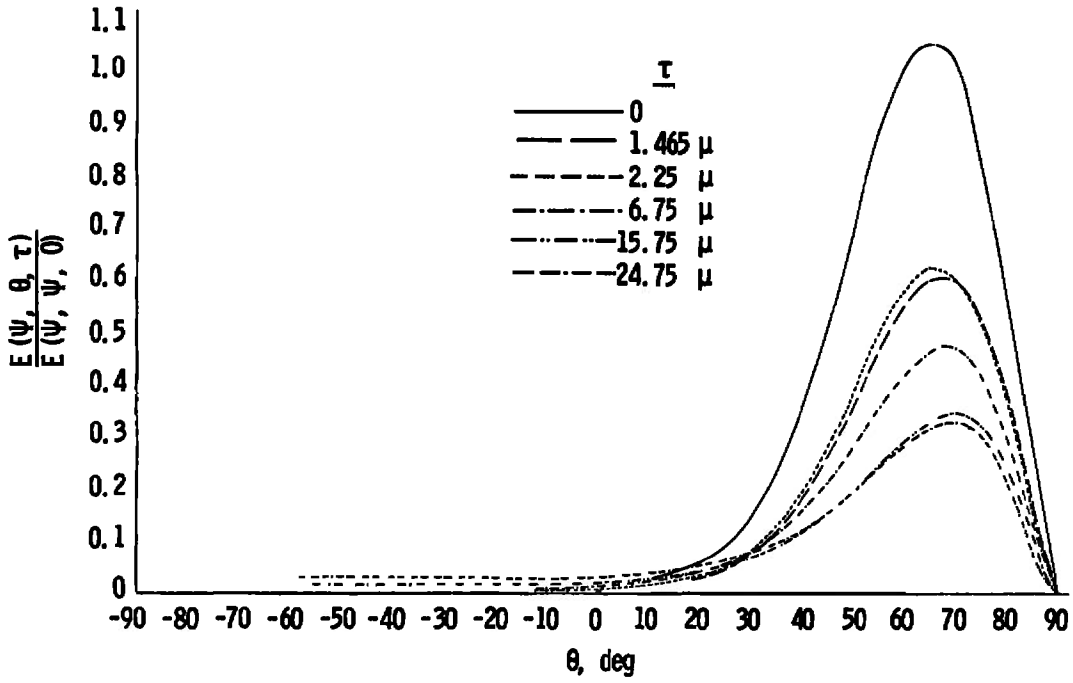

g. ψ = 60 deg

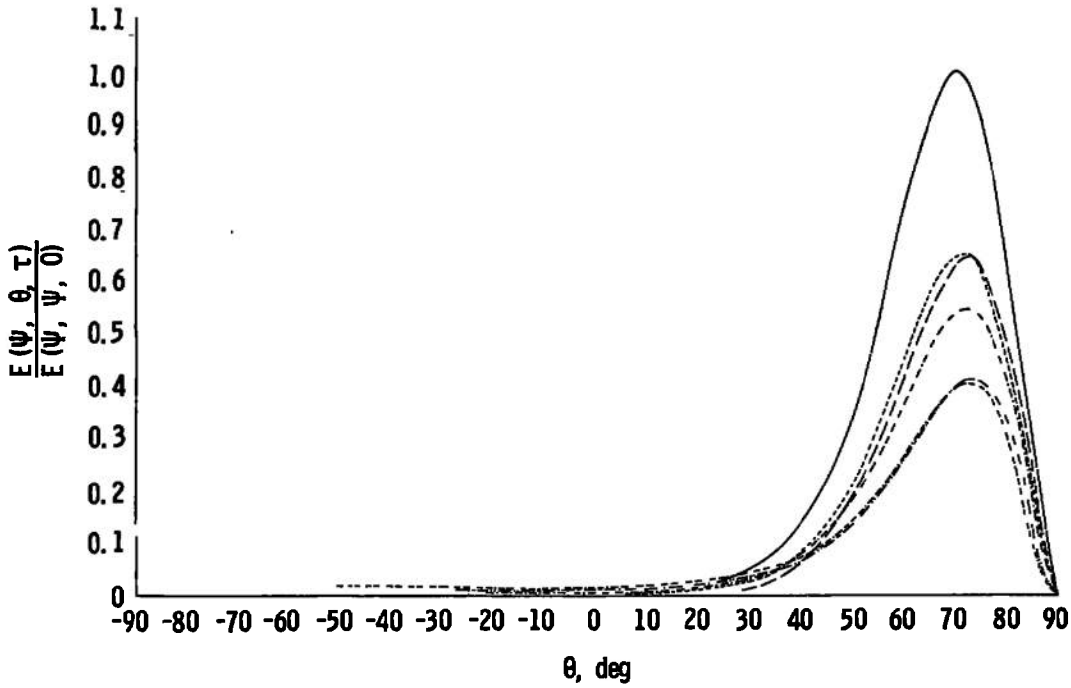

h. ψ = 70 deg

Fig. 11 Concluded

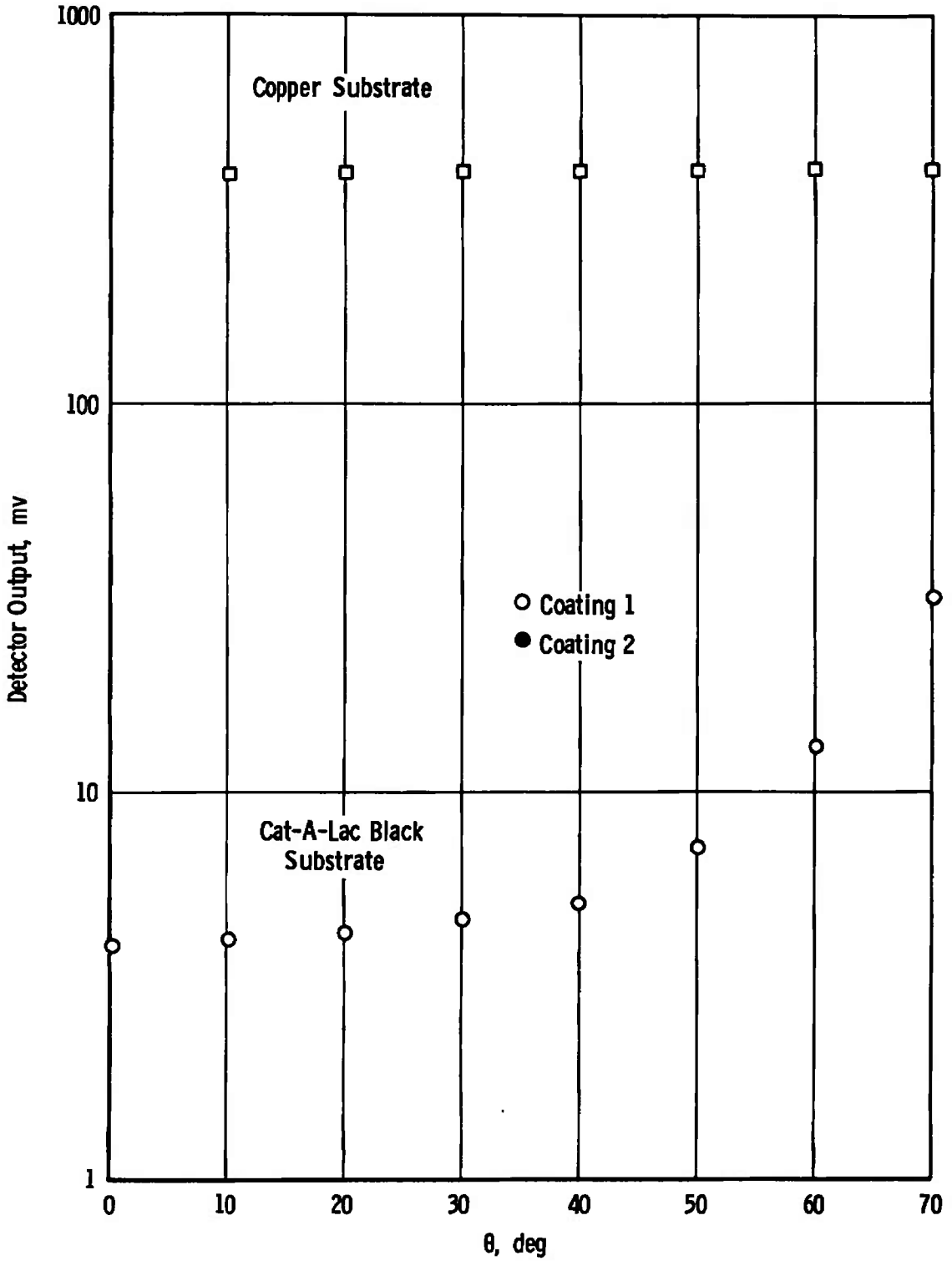

Fig. 12 Detector Output at $\theta = \psi$ for a 300°K Surface without Cryodeposit Used to Normalize Data

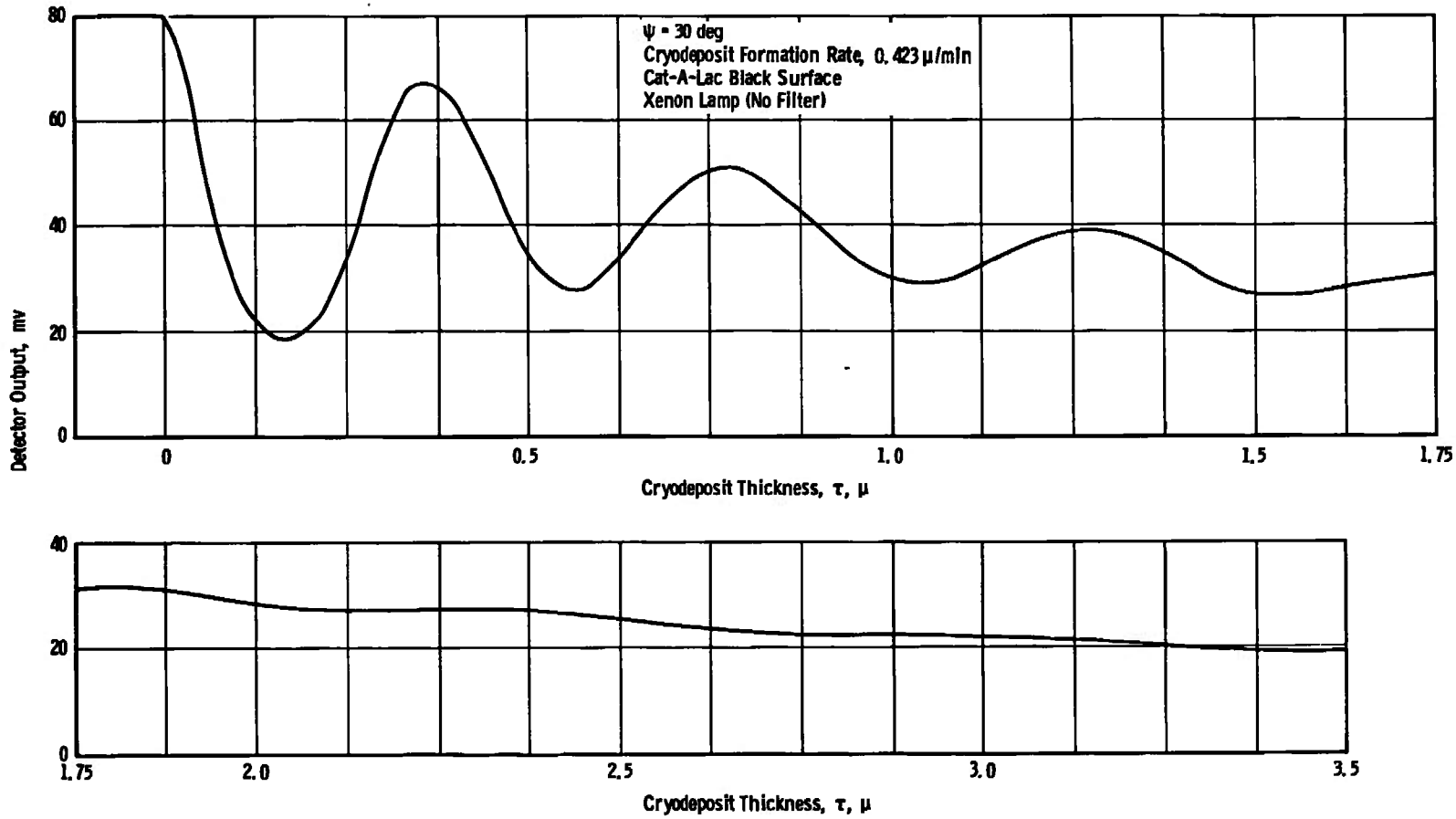

Fig. 13 Bragg Interference Patterns with a White-Light Source

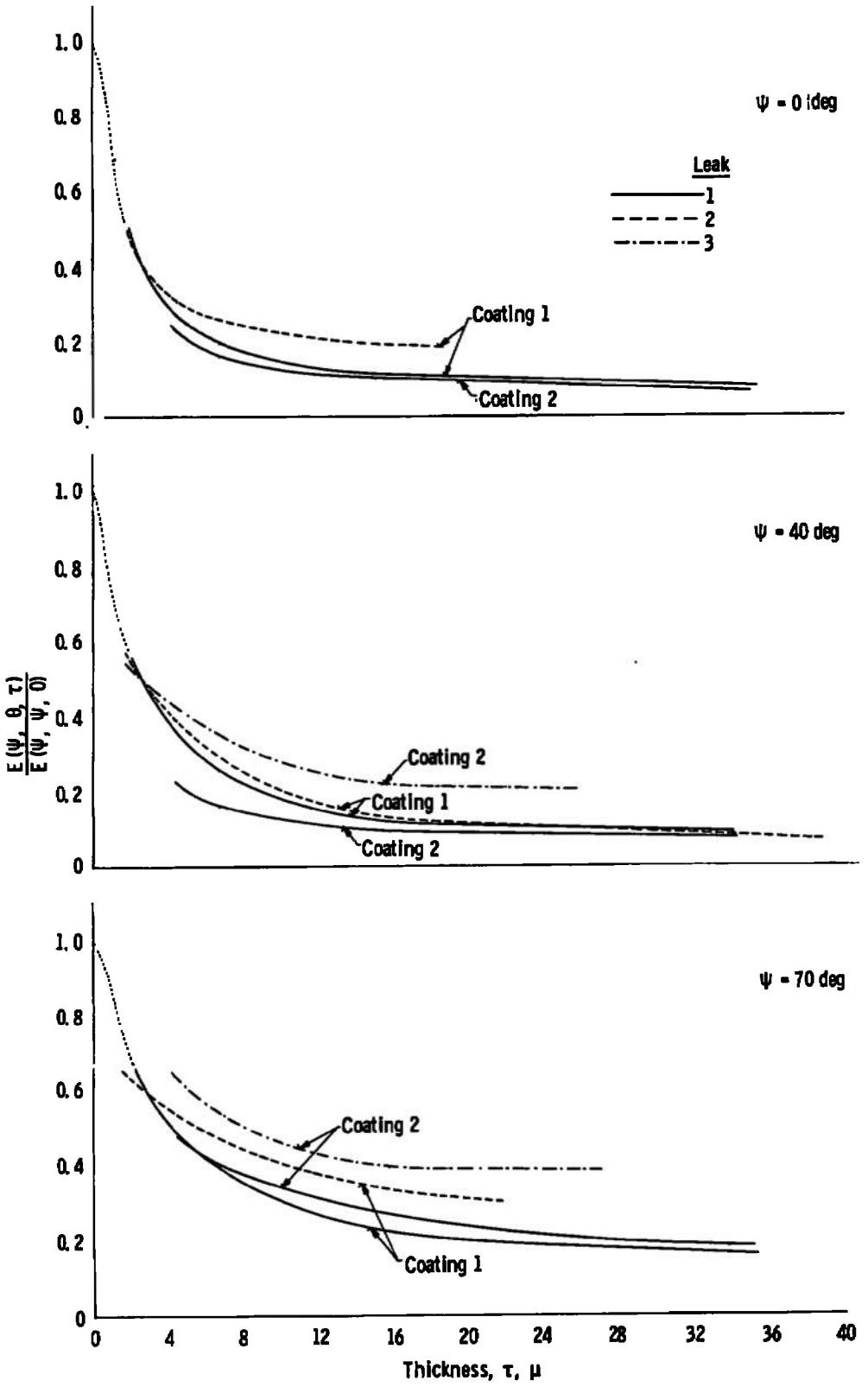

Fig. 14 Variation of Normalized Reflected Energy Output at Specular Angle for Various CO_2 Cryodeposits Formed on Two Different Cat-A-Lac Black Surfaces

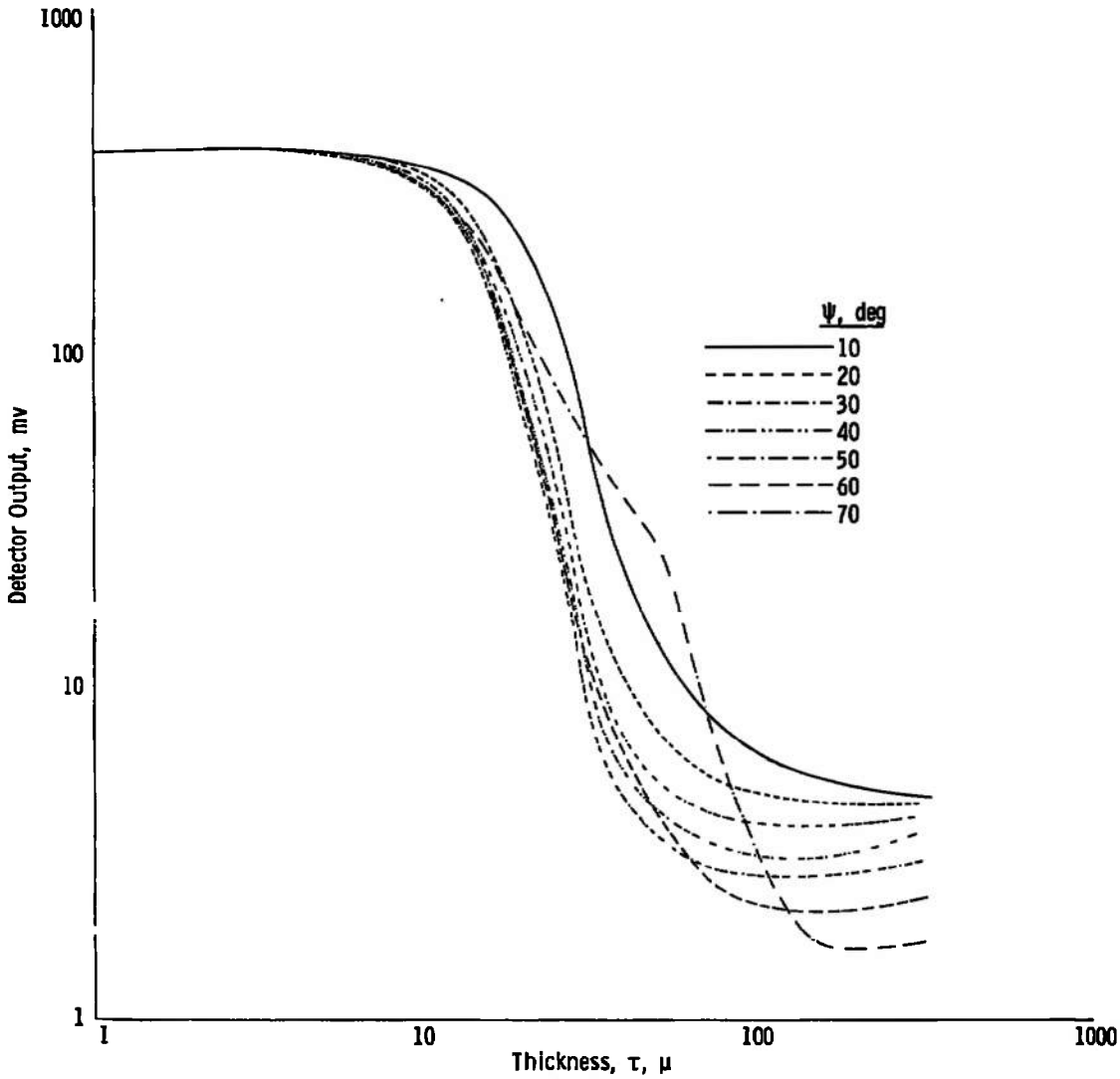

Fig. 15 Variation of Reflected Energy at Specular Angle from CO_2 Cryodeposits Formed at 2.25 μ/min on a Polished Copper Substrate

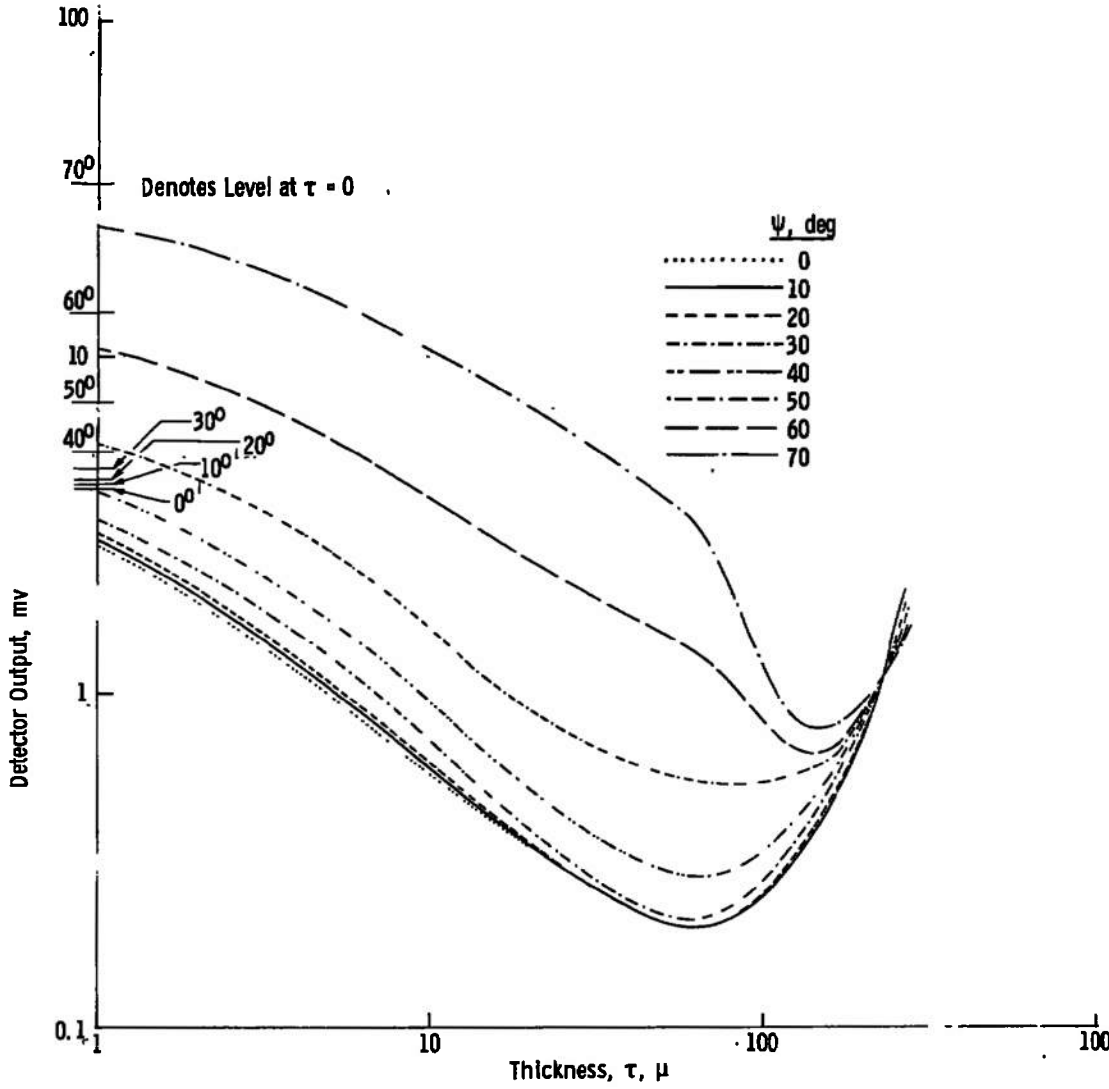

Fig. 16 Variation of Reflected Energy at Specular Angle from CO_2 Cryodeposits Formed at 2.25 μ/min on a Black Epoxy Painted Substrate

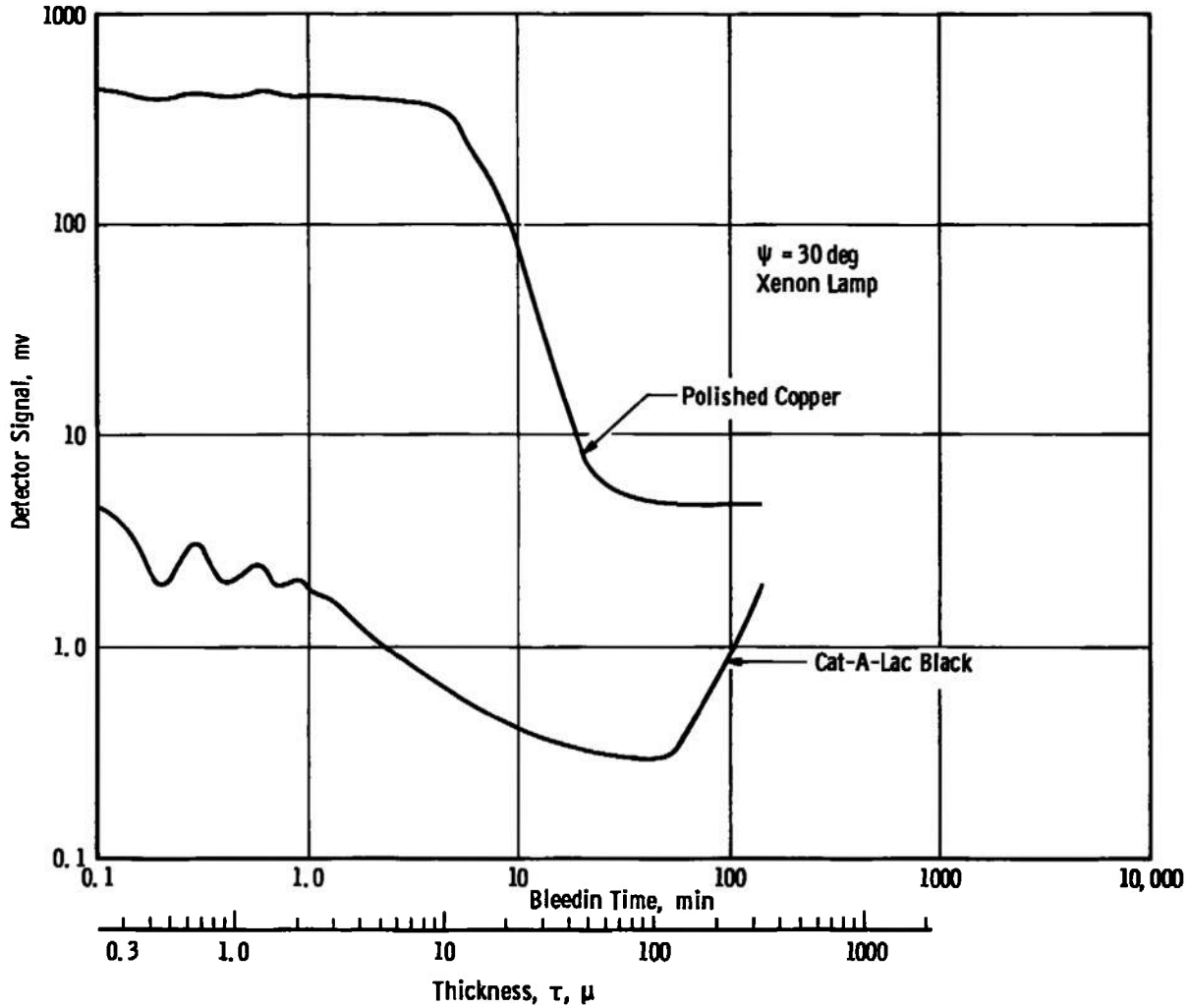

Fig. 17 Comparison of Light Reflected from CO_2 Cryodeposits on Polished Copper and Black Epoxy Painted Substrates at the Specular Angle of Reflection

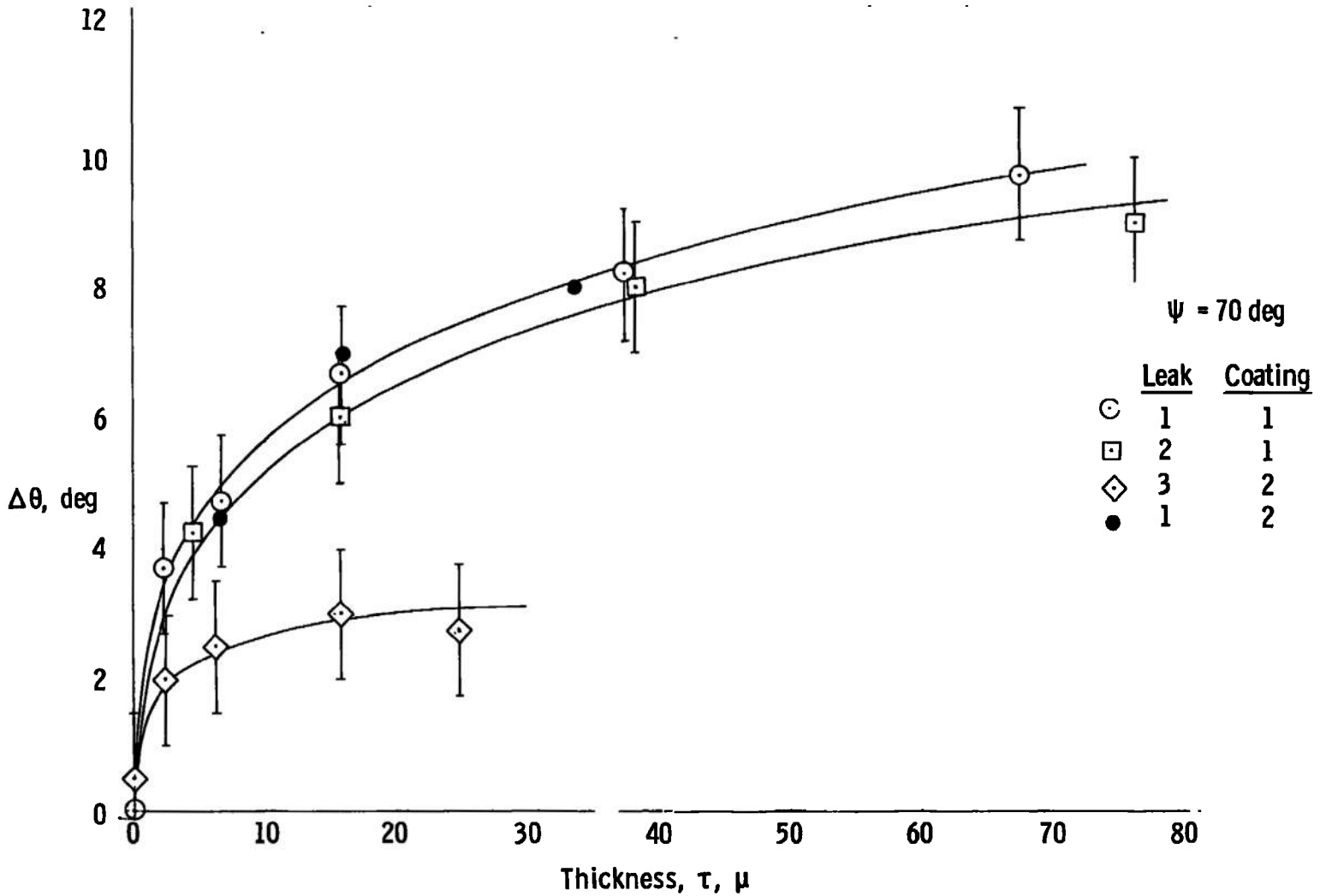

Fig. 18 Angular Shift of the Specular Component of Light Reflected from CO_2 Cryodeposits Formed at Various Rates on a Black Epoxy Painted Substrate

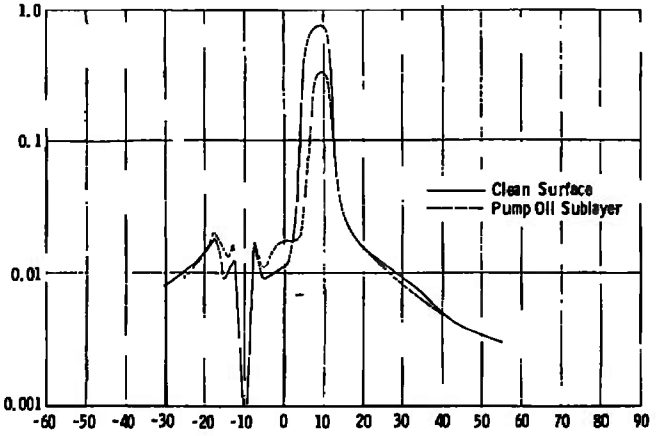

a. ψ = 10 deg, θ = 0 deg, τ = 15.75 μ

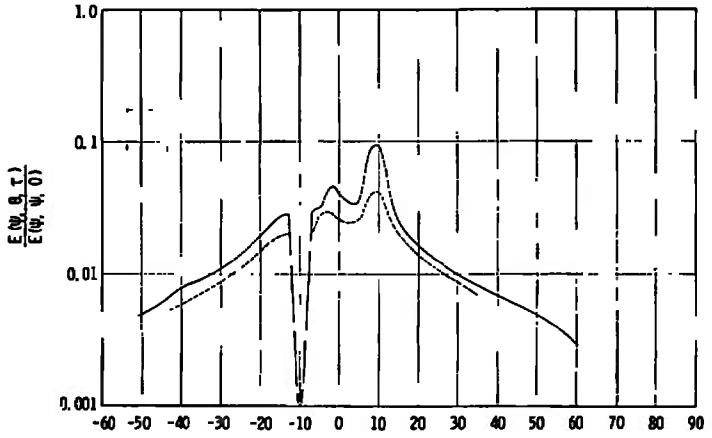

b. ψ = 10 deg, θ = 0 deg, τ = 33.75 μ

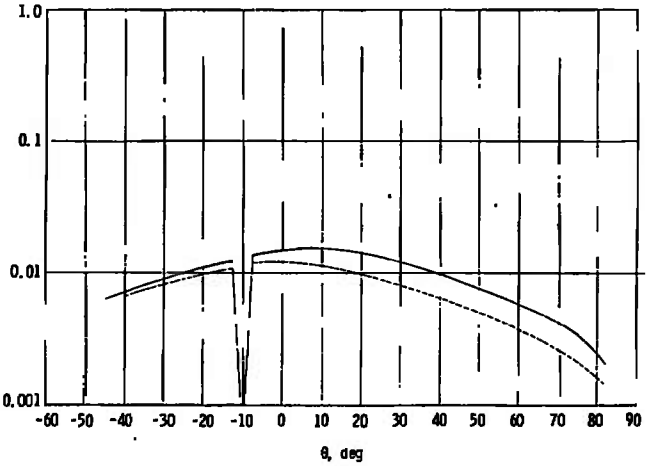

c. ψ = 10 deg, θ = 0 deg, τ = 122.5 μ

Fig. 19 Comparison of the Distribution of Light Reflected by CO_2 Cryodeposits Formed on a Polished Copper Surface with and without an Oil Frost Sublayer

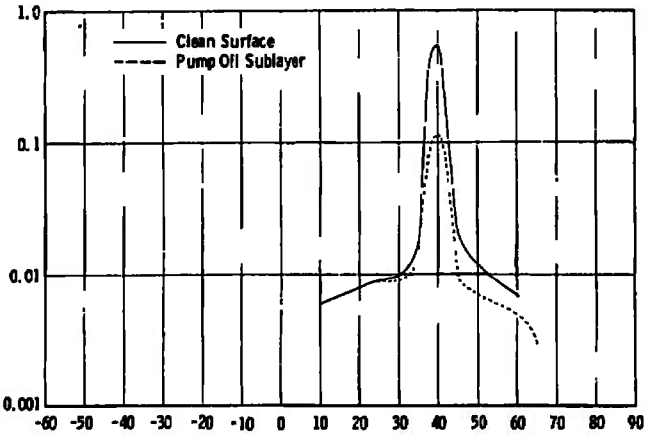

d. ψ = 40 deg, ϕ = 0 deg, r = 15.75 μ

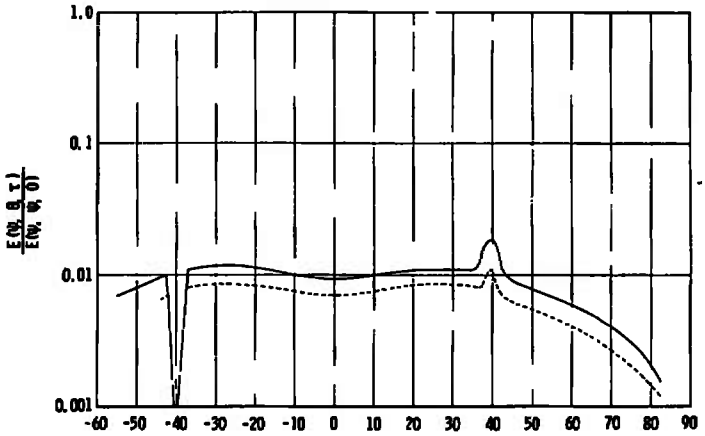

e. ψ = 40 deg, ϕ = 0 deg, r = 33.75 μ

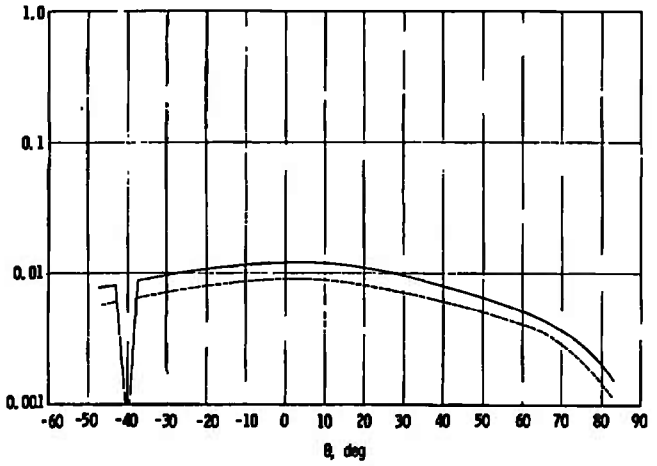

f. ψ = 40 deg, ϕ = 0 deg, r = 122.5 μ

Fig. 19 Concluded

UNCLASSIFIED
Security Classification

DOCUMENT CONTROL DATA - R & D

(Security classification of title, body of abstract and indexing annotation must be entered when the overall report is classified)

1. ORIGINATING ACTIVITY (Corporate author)	2a. REPORT SECURITY CLASSIFICATION
Arnold Engineering Development Center, ARO, Inc., Operating Contractor, Arnold AF Station, Tennessee	UNCLASSIFIED
	2b. GROUP N/A

3. REPORT TITLE

ANGULAR DISTRIBUTION OF RADIATION REFLECTED FROM CARBON DIOXIDE CRYODEPOSITS FORMED ON 77°K SURFACES

4. DESCRIPTIVE NOTES (Type of report and inclusive dates)

June 1967 to January 1968 - Final Report

5. AUTHOR(S) (First name, middle initial, last name)

Thermal Radiation Section, ARO, Inc.

6. REPORT DATE	7a. TOTAL NO. OF PAGES	7b. NO. OF REFS
April 1968	61	9

8a. CONTRACT OR GRANT NO. AF40(600)-1200	9a. ORIGINATOR'S REPORT NUMBER(S)
b. PROJECT NO. 8951	AEDC-TR-68-46
c. Program Element 6240533F	9b. OTHER REPORT NO(S) (Any other numbers that may be assigned this report)
d. Task 895104	N/A

10. DISTRIBUTION STATEMENT

This document has been approved for public release and sale; its distribution is unlimited.

11. SUPPLEMENTARY NOTES	12. SPONSORING MILITARY ACTIVITY
Available in DDC.	Arnold Engineering Development Center (AETS), Air Force Systems Command, Arnold AF Station, Tennessee

13. ABSTRACT

The angular distribution of light reflected from carbon dioxide cryodeposits formed at various rates on polished copper and black substrates has been measured for various cryodeposit thicknesses and angles of incidence. Cryodeposits were found to reflect light essentially diffusely at thicknesses greater than about 100 microns (μ). The specular reflection from both polished copper and black substrates could be reduced by as much as two orders of magnitude by a 100-μ-thick cryodeposit. Bragg interference, backscattering, scattering interference, and shifts of the angular location of the specular component were all observed and illustrated that light reflection from cryodeposits is a very complex phenomenon.

DD FORM 1 NOV 65 1473

UNCLASSIFIED
Security Classification

14. KEY WORDS	LINK A		LINK B		LINK C	
	ROLE	WT	ROLE	WT	ROLE	WT
1 cryodeposits						
2 carbon dioxide						
black painted 3 substrates						
polished copper substrates						
light reflection						
Bragg interference						
4 backscattering						
scattering interference						
specular component shifts						

15-2